PTEP

Prog. Theor. Exp. Phys. **2018**, 063B04 (35 pages)
DOI: 10.1093/ptep/pty062

# Commutative geometry for non-commutative D-branes by tachyon condensation

Tsuguhiko Asakawa[1,*], Goro Ishiki[2,3,*], Takaki Matsumoto[3,*], So Matsuura[4,*], and Hisayoshi Muraki[5,*]

[1]*Department of Integrated Design Engineering, Maebashi Institute of Technology, Maebashi 371-0816, Japan*
[2]*Tomonaga Center for the History of the Universe, University of Tsukuba, Tsukuba, Ibaraki 305-8571, Japan*
[3]*Graduate School of Pure and Applied Sciences, University of Tsukuba, Tsukuba, Ibaraki 305-8571, Japan*
[4]*Department of Physics, Hiyoshi Campus, and Research and Education Center for Natural Science, Keio University, 4-1-1 Hiyoshi, Yokohama 223-8521, Japan*
[5]*Department of Physics, Sogang University, Seoul 04107, Korea*
[*]E-mail: asakawa@maebashi-it.ac.jp, ishiki@het.ph.tsukuba.ac.jp, matsumoto@het.ph.tsukuba.ac.jp, s.matsu@phys-h.keio.ac.jp, hmuraki@sogang.ac.kr

Received March 31, 2018; Revised May 2, 2018; Accepted May 2, 2018; Published June 20, 2018

There is a difficulty in defining the positions of the D-branes when the scalar fields on them are non-Abelian. We show that we can use tachyon condensation to determine the position or the shape of D0-branes uniquely as a commutative region in spacetime together with a non-trivial gauge flux on it, even if the scalar fields are non-Abelian. We use the idea of the so-called coherent state method developed in the field of matrix models in the context of the tachyon condensation. We investigate configurations of non-commutative D2-brane made out of D0-branes as examples. In particular, we examine a Moyal plane and a fuzzy sphere in detail, and show that whose shapes are commutative $\mathbb{R}^2$ and $S^2$, respectively, equipped with uniform magnetic flux on them. We study the physical meaning of this commutative geometry made out of matrices, and propose an interpretation in terms of K-homology.

Subject Index B23, B26, B82, B83

## 1. Introduction

D-branes in superstring theory are dynamical hypersurfaces in spacetime on which gauge fields and transverse scalar fields live. On a single D-brane, the transverse scalar fields represent the displacement of the worldvolume in spacetime. However, this interpretation cannot be applied naively for a stack of $N$ D-branes, since the scalar fields take values in $N \times N$ Hermitian matrices, which are not mutually diagonalizable in general. Soon after the discovery of D-branes, the idea that such non-commuting scalar fields represent non-commutative (NC) geometry [1,2] came out. It is most readily seen by the matrix quantum mechanics for multiple D0-branes [3] or the matrix model [4], which is (at least formally) seen as a model for D-instantons. According to this matrix geometry picture, various NC configurations of scalar fields, representing NC spaces such as the Moyal plane [5] and the fuzzy sphere [6] are considered. In these examples, the non-Abelian scalar fields on lower-dimensional D-branes make the system couple to the Ramond–Ramond (RR) 3-form potential due to the Myers term and the effective theories on them become NC gauge theories. Here there appears a puzzle: Such an NC worldvolume lives in the usual commutative spacetime while an NC space cannot be embedded into commutative spacetime in the usual sense in general. Therefore, the position or the shape of an NC D-brane in the commutative spacetime is far from obvious in particular.


Funded by SCOAP[3]

This problem has been discussed from various viewpoints. In Ref. [7], the position of NC D-brane systems is estimated as the distribution of D-brane charges by using the D-brane charge density formula given in Refs. [8,9]. The original charge density formula is improved by assuming that fuzzy sphere configurations have single spherical shell structures, which gives a consistent improvement of the formula. This suggests that the worldvolume of the NC D-brane system has a definite shape in the spacetime.

The way to determine the shape of the D-brane system is not unique. The original interpretation that the diagonal elements of the scalar fields express the position of the worldvolume in spacetime has been generalized in Ref. [10], where the authors discuss the concept that the position of the worldvolume should be identified by taking the "almost diagonal gauge" [11] of the scalar fields.

In Ref. [12], another interesting method of defining the shape of NC D-branes was proposed. In this method, in addition to NC D-branes, one introduces a probe D0-brane and considers open strings connecting the probe brane and the NC D-branes. The point is that the lowest energy of an open string is always proportional to the length of the string. Then, moving the position of the probe brane, one can find massless modes of an open string only when the probe brane hits the NC branes so that the length of one of the open strings becomes zero. Thus, the set of all possible positions of the probe brane such that the open strings have massless modes can be interpreted as the shape of the NC branes. The energy of the open string can be measured by using a Dirac operator on the open strings and thus the shape of the NC branes is defined as the loci of zeros of the Dirac operator. See Refs. [13,16] for analysis of this method. See also Refs. [14,15] for NC spheres in the Berenstein-Maldacena-Nastase (BMN) matrix model.

The relation between NC and commutative geometries has been further developed as a mathematical correspondence between commutative geometry and matrices. In Ref. [17], a systematic way to extract a commutative space from a given configuration of matrices has been developed. In this approach, a Hamiltonian operator plays an important role, which is assumed to include matrices accompanied by coordinates of a Euclidean space $\mathbb{R}^n$ as parameters. The commutative manifold living in $\mathbb{R}^n$ is identified as the loci of zero eigenstates of the Hamiltonian, and some geometrical quantities such as Poisson structures and Riemannian metrics can also be extracted by the coherent states [17] (see also Ref. [18]). Although the large-$N$ limit of the matrices has been considered in Ref. [17], it has been pointed out in Ref. [19] that this idea works even at finite $N$ with the use of quasi-coherent states, and it has been discussed that a Dirac-like operator can play the same role as the Hamiltonian. Interestingly enough, the obtained formulation is deeply related to that developed in the context of the superstring theory discussed in Ref. [12]. We thus refer to the method developed in Refs. [12,17,19] collectively as the "coherent state method" hereafter. See also Ref. [20] for the connection between coherent states and the fuzzy sphere.

In this paper, we point out that the coherent state method also plays important roles in the context of tachyon condensation in superstring theory [21,22]. The basic idea is to identify the Dirac-like operator in the coherent state method with a tachyon profile on a system of unstable D-branes. With this identification, the coherent state method can be interpreted as the tachyon condensation, and the resultant commutative manifolds can be regarded as D-branes living in the commutative spacetime. The advantage of this interpretation is twofold: First, the parameter space $\mathbb{R}^n$ in the coherent state method can be interpreted as a worldvolume of these unstable D-branes. Second, it gives a clear reason why the ground state should be chosen to extract the commutative worldvolume.

Technically our analysis in this paper is an application of the technique developed so far [23]. This method has been applied to realize the Nahm construction of monopoles and the

Atiyah-Drinfeld-Hitchin-Manin (ADHM) construction of instantons [24,25] and/or to realize a spherical D-brane [26]. In the latter case, a system of 2 non-BPS D3-branes is considered, where a tachyon profile $T$ representing a D0-brane is deformed by a constant shift. By diagonalizing the tachyon $T$, the system is shown to condensate to a spherical D2-brane with a gauge flux of the unit monopole charge. Since the diagonalization is just a change of basis, the original deformed D0-brane and the spherical D2-brane with flux are unitarily equivalent. This construction is similar but different from the well-known Myers dielectric D2-brane. In the former case, a D2-brane is made out of a single D0-brane and its worldvolume is a commutative $S^2$, while in the latter case a D2-brane is made out of multiple D0-branes and its worldvolume is a fuzzy sphere. In this paper, we apply tachyon condensation to the latter case and show that the fuzzy sphere has an equivalent expression to a system on a commutative sphere. For the latest result in the related topic, see Ref. [27], which has some overlap with the present paper and appeared on arXiv at the same time as the present paper.

The organization of this paper is as follows. In Sect. 2, we consider the system of $k$ D0-branes with matrix-valued scalar fields on them, in terms of a tachyon field of $2k$ non-BPS D3-branes. By using the idea of the coherent state method in this setting, we claim that the shape of D0-branes is a commutative region $M$ of spacetime, and is determined uniquely by the zeros of the tachyon field. We also explain a general mechanism of producing a gauge flux on $M$. In Sect. 3, we apply the method to NC D2-branes on the Moyal plane and the fuzzy sphere, which are made of D0-branes with the Myers term. We identify the shapes of these systems as *commutative* $\mathbb{R}^2$ and $S^2$, respectively. In Sect. 4, we discuss the meaning of the shapes in more detail and propose an interpretation in terms of K-homology. Section 5 is devoted to the conclusion and discussion.

## 2. Geometry from matrices by tachyon condensation

### 2.1. *Multiple D0-branes in non-BPS D-branes*

Consider a system of $N$ non-BPS D3-branes whose worldvolume is $\mathbb{R} \times \mathbb{R}^3$ in 10D Minkowski spacetime. The effective action is a $U(N)$ gauge theory coupled with 6 transverse scalar fields and a tachyon field. In this paper, we focus on static configurations of the tachyon field only. We also restrict the gauge connection to be trivial. In this setting, D3-branes are rigid and their spatial worldvolume is identified with part of the spacetime. We set the spatial coordinates $\boldsymbol{x} = (x^1, x^2, x^3)$. Moreover, the Chan–Paton bundle, a complex vector bundle over $\mathbb{R}^3$ with the fiber $\mathbb{C}^N$, is trivial $\mathbb{R}^3 \times \mathbb{C}^N$ because of the lack of gauge field. The tachyon field $T(\boldsymbol{x})$ is a Hermitian $N \times N$-matrix-valued scalar field.

Our argument below does not rely on the explicit form of the action, but for definiteness, we assume the that tachyon potential has the form $V(T) = e^{-T^2}$ (i.e., we assume boundary string field theory (BSFT) type theory [28,29]). Because it is unstable around the (false) vacuum $T = 0$, tachyon condensation occurs. At the true vacuum $T = u1_N$ ($u \to \infty$), non-BPS D3-branes disappear. In addition, lower-dimensional D-branes can be realized as solitonic configurations [21,22].

Among them, let us consider $k$ D0-brane configuration with fluctuations. We take $N = 2k$ and set the tachyon profile as

$$T(\boldsymbol{x}) = u\boldsymbol{\sigma} \cdot (\boldsymbol{x} - \Phi) = u \begin{pmatrix} x^3 - \Phi^3 & \bar{z} - \bar{\Phi} \\ z - \Phi & -x^3 + \Phi^3 \end{pmatrix}, \tag{2.1}$$

where $\boldsymbol{\sigma} = (\sigma^1, \sigma^2, \sigma^3)$ is a set of Pauli matrices and $\Phi = (\Phi^1, \Phi^2, \Phi^3)$ is a collection of transverse scalar fields on $k$ D0-branes that are $k \times k$ Hermitian matrices. In the second expression, we used

complex notation with $z = x^1 + ix^2$ and $\Phi = \Phi^1 + i\Phi^2$. Note that $x^i$ should be understood as $x^i \otimes \mathbf{1}_k$ more precisely.

The tachyon profile (2.1) without fluctuation, $\Phi = 0$, indeed represents $k$ D0-branes sitting at the origin $\boldsymbol{x} = 0$ in the limit $u \to \infty$, which is known as the Atiyah–Bott–Shapiro (ABS) construction [30,31]. This is essentially seen by the tachyon potential

$$V(T) = e^{-T^2} = e^{-u^2|\boldsymbol{x}|^2} \otimes \mathbf{1}_{2k}, \tag{2.2}$$

which is proportional to the delta function $\delta(\boldsymbol{x})$ in the $u \to \infty$ limit. Thus, under tachyon condensation, the spatial worldvolume $\mathbb{R}^3$ reduces to the origin, leaving a point-like defect. This fact is most rigorously shown by using boundary states (see, e.g., Ref. [32]): The boundary state for non-BPS D3-branes with this tachyon profile added on as a boundary interaction reduces to the boundary state for $k$ D0-branes in the limit $u \to \infty$, with the correct tension and the RR-charge. Even adding fluctuations, the profile (2.1) reduces to $k$ D0-branes with transverse scalars, where scalar fields appear as a boundary interaction. The resulting effective action $S_{\mathrm{D0}}[\Phi]$ for $k$ D0-branes is given by the Dirac–Born–Infeld (DBI) action and the Chern–Simons term, which in particular includes the Myers term [6]. In the opposite way, a matrix model $S_{\mathrm{D0}}[\Phi]$ can be embedded into the theory of non-BPS D3-branes. This explains why the tachyon field appears when considering the shape of D-branes with non-commuting scalar fields.

Note that, in this treatment, the condensation itself is obtained without matrix scalar fields $\Phi$, and $\Phi$ are turned on afterwards as perturbation. An equivalent but more direct way is to consider the condensation of the profile (2.1) with $\Phi$. The resulting defect should be the deformation of the point-like defect by matrices $\Phi$. Indeed, as shown in Ref. [26], a deformation of the single D0-brane ($k = 1$) profile drastically changes the condensation defect to a spherical D2-brane[1]. Our claim in this paper is that the position or the shape of D-branes is determined by diagonalizing the tachyon field $T$, not the scalar fields $\hat{\mathrm{I}}_i$ themselves. The point is that diagonalizing a tachyon profile is always possible for any matrix-valued scalar fields $\Phi$. As a result, the shape is irrespective of whether or not the system is a classical solution of the effective theory of D0-branes and/or supergravity.

In the following, we will consider such configurations of matrix scalar fields $\Phi$ that represent non-commutative D2-branes as typical examples. In particular, we investigate an NC plane and a fuzzy sphere in detail. By embedding D0-branes into non-BPS D3-branes, we will see that the spatial worldvolume $\mathbb{R}^3$ shrinks to a commutative 2D space after tachyon condensation. Moreover, this process inevitably induces a non-trivial gauge field, whose field strength carries the D0-brane charge $k$.

### 2.2. *Tachyon condensation and gauge flux production*

Before treating explicit examples, we describe the schematic structure of the tachyon condensation for the configuration (2.1). Technically, the analysis is the same as the coherent state method mentioned in the introduction. We also explain how a non-trivial $U(1)$ gauge flux is induced from the tachyon condensation. In order to consider the case of not only finite but also infinite $N$, we formulate the problem in terms of Hilbert spaces and projective modules.

[1] It is a deformation of Eq. (2.1) with $\Phi = 0$ by a constant shift and thus different from $\Phi$ here.

### 2.2.1. *Tachyon condensation*

The Chan–Paton bundle for $N$ non-BPS D3-branes in our setting is a trivial complex vector bundle $E = \mathbb{R}^3 \times \mathbb{C}^N$ over $\mathbb{R}^3$, whose typical fiber $\mathbb{C}^N$ is a Hilbert space. Then, the space of sections of the Chan–Paton bundle is a free module $\mathcal{A}^N$ of rank $N$, with $\mathcal{A} = C^\infty(\mathbb{R}^3)$. Denote an orthonormal basis (ONB) for $\mathbb{C}^N$ as $|\, a \,\rangle$ $(a = 0, 1, 2, \ldots, N-1)$. Then, a generic section is written as

$$|\, \psi(\boldsymbol{x}) \,\rangle = \sum_{a=0}^{N-1} \psi^a(\boldsymbol{x}) \,|\, a \,\rangle, \quad \psi^a(\boldsymbol{x}) = \langle\, a \,|\, \psi(\boldsymbol{x}) \,\rangle \in \mathcal{A}. \tag{2.3}$$

The tachyon field $T(\boldsymbol{x})$ is an operator-valued function on $\mathbb{R}^3$. It is an element of the endomorphism $\mathrm{End}(E)$ and is written as $T(\boldsymbol{x}) = \sum_{a,b} |\, a \,\rangle\, T_b^a(\boldsymbol{x})\, \langle\, b \,|$. According to Eq. (2.1), we assume that each matrix element $T_b^a$ is at order $u$, and the limit $u \to \infty$ will be taken. Note that in this profile (2.1), the matrices $\Phi$ act at each $\boldsymbol{x}$ (not only at the origin).

In order to extract the condensation defect, we need to diagonalize the potential $V(T) = e^{-T^2}$ or the tachyon field $T(\boldsymbol{x})$ itself at each point $\boldsymbol{x}$ on $\mathbb{R}^3$. Any Hermitian matrix can be diagonalized by a unitary matrix. In an infinite-dimensional Hilbert space and operators acting on it, the corresponding notion is the spectral decomposition. Assuming spectral decomposition at each point $\boldsymbol{x}$,

$$T(\boldsymbol{x}) = U(\boldsymbol{x}) T_0(\boldsymbol{x}) U(\boldsymbol{x})^\dagger, \quad T_0(\boldsymbol{x}) = \sum_a |\, a \,\rangle\, t_a(\boldsymbol{x})\, \langle\, a \,|, \tag{2.4}$$

we find the eigenstates for the tachyon field as

$$T(\boldsymbol{x}) \,|\, \psi_a(\boldsymbol{x}) \,\rangle = t_a(\boldsymbol{x}) \,|\, \psi_a(\boldsymbol{x}) \,\rangle, \quad |\, \psi_a(\boldsymbol{x}) \,\rangle = U(\boldsymbol{x}) \,|\, a \,\rangle. \tag{2.5}$$

Here an eigenstate $|\, \psi_a(\boldsymbol{x}) \,\rangle$, which is a section of the Chan–Paton bundle, and the unitary operator $U(\boldsymbol{x})$ are position-dependent. In more familiar terms, Eq. (2.4) is a gauge transformation of the tachyon field. In general, eigenfunctions $t_a(\boldsymbol{x})$ are $u$-dependent but $U(\boldsymbol{x})$ is $u$-independent (see the examples below).

Then, the tachyon potential is written as

$$e^{-T^2} = U(\boldsymbol{x}) e^{-T_0(\boldsymbol{x})^2} U(\boldsymbol{x})^\dagger = \sum_a U(\boldsymbol{x}) \,|\, a \,\rangle\, e^{-t_a(\boldsymbol{x})^2}\, \langle\, a \,|\, U(\boldsymbol{x})^\dagger. \tag{2.6}$$

This shows that, at each $\boldsymbol{x}$, the component with $t_a(\boldsymbol{x}) \neq 0$ tends to 0 in the limit $u \to \infty$. That is, the tachyon potential picks up tachyon zero modes at each point. For example[2], if only one component is the zero mode $t_0(\boldsymbol{x}) = 0$ for any $\boldsymbol{x}$, then

$$e^{-T^2} \to P(\boldsymbol{x}) = U(\boldsymbol{x}) \,|\, 0 \,\rangle\, \langle\, 0 \,|\, U(\boldsymbol{x})^\dagger. \tag{2.7}$$

In this case, all the excited states $|\, a \,\rangle$ $(a \neq 0)$ are annihilated under the tachyon condensation. Note that $P_0 = |\, 0 \,\rangle\, \langle\, 0 \,|$ is a rank-1 projection operator acting on the typical fiber, and the $P(\boldsymbol{x})$ is unitarily equivalent to $P_0$. This means that the tachyon condensation picks up a 1D subspace $U(\boldsymbol{x}) \,|\, 0 \,\rangle$ from the $N$-dimensional fiber at each point $\boldsymbol{x}$. More generally, it may happen that $t_0(\boldsymbol{x}) = 0$ for some region $M \subset \mathbb{R}^3$, but $t_0(\boldsymbol{x}) \neq 0$ otherwise. In this case, the tachyon potential also projects out from the region $M$. Schematically,

$$e^{-T^2} \to \delta(M) P(\boldsymbol{x}) = \delta(M) U(\boldsymbol{x}) \,|\, 0 \,\rangle\, \langle\, 0 \,|\, U(\boldsymbol{x})^\dagger, \tag{2.8}$$

[2] This is just a working assumption. More general situations are discussed in Sect. 5.

where $\delta(M)$ denotes a delta function distribution with its support on $M$. The original information on the choice of matrices $\Phi$ in Eq. (2.1) is transferred to two kinds of information, $\delta(M)$ and $P(\boldsymbol{x})$.

Note that this procedure is completely point-wise, and in general the unitary operator $U(\boldsymbol{x})$ is not globally defined as a smooth function on the whole $\mathbb{R}^3$. For such cases, we may apply the procedure by considering it as patch-wise. That is, choose an open covering $\{\mathcal{U}_I\}$ of $\mathbb{R}^3$, such that the corresponding set of unitary operators $\{U_I(\boldsymbol{x})\}$ are defined smoothly on each $\mathcal{U}_I$. For a point in the overlap $\mathcal{U}_I \cap \mathcal{U}_J$, there are two diagonalizations but they give the same defect because the eigenfunction $t_0(\boldsymbol{x})$ is gauge-independent. Then, the region $M$ is also given patch-wise by the union $M = \cup_I M_I$. Our examples below are of the type (2.8) with $M = \mathbb{R}^2$ and $M = S^2$. In the latter case, patch-wise condensation is needed. In these cases, a defect after the condensation is interpreted as a D2-brane on $M$. What kind of $M$ appears depends of course on the choice of the matrices $\Phi$.

In summary, the tachyon condensation just picks up the zeros of the eigenfunction and as a result a defect remains on a region $M$. This is technically the same as the coherent state method mentioned in the introduction. In fact, the tachyon profile $T$ (2.1) is exactly the same as the Dirac-like operator in the literature [12,13,16,19] and $T^2$ corresponds to the Hamiltonian in Refs. [17,18]. Our claim in this paper is that the tachyon condensation gives a new physical interpretation of this prescription, based on the dynamics of the non-BPS D-branes. Although we are working with static configurations, the condensation is essentially a dynamical process and the zero modes survive as a result of the dynamics. This is in contrast with the previously proposed interpretations in Refs. [12,17,19] of the coherent state method, which are based on statics.

### 2.2.2. *Gauge flux production*

A tachyon potential of the form (2.7) or (2.8) induces a $U(1)$-flux. We here briefly describe the mechanism of this effect. For more details we refer the reader to Ref. [26].

On the Chan–Paton bundle, the tachyon potential (2.7) plays the role of a projection operator $P(\boldsymbol{x})$, which picks up a subspace $U(\boldsymbol{x})\,|\,0\,\rangle$ at each fiber. This defines a projective module $P\mathcal{A}^N$, which is identified as the space of sections of a line bundle on $\mathbb{R}^3$. Since $U(\boldsymbol{x})$ is a unitary operator, $U(\boldsymbol{x})\,|\,a\,\rangle$ forms an orthonormal basis at each fiber. We may then write a generic element of the free module $\mathcal{A}^N$ in this new basis as

$$|\,\psi(\boldsymbol{x})\,\rangle = \sum_a \psi^a(\boldsymbol{x}) U(\boldsymbol{x})\,|\,a\,\rangle. \tag{2.9}$$

An element of the projective module $P\mathcal{A}^N$ is then given by

$$P(\boldsymbol{x})\,|\,\psi(\boldsymbol{x})\,\rangle = \psi^0(\boldsymbol{x}) U(\boldsymbol{x})\,|\,0\,\rangle. \tag{2.10}$$

Since $P(\boldsymbol{x})$ depends on $\boldsymbol{x}$, the exterior derivative $d$ does not preserve the module $P\mathcal{A}^N$ in general. This leads to the notion of connections. A natural connection on $P\mathcal{A}^N$, called the Grassmannian connection, is defined by $\nabla = P \circ d$, which acts as

$$\begin{aligned} Pd(P\,|\,\psi\,\rangle) &= Pd(\psi^0 U\,|\,0\,\rangle) \\ &= P(d\psi^0 U\,|\,0\,\rangle + \psi^0 dU\,|\,0\,\rangle) \\ &= d\psi^0 U\,|\,0\,\rangle + \psi^0 U\,|\,0\,\rangle\,\langle\,0\,|\,U^\dagger dU\,|\,0\,\rangle \\ &= \left(d\psi^0 + iA\psi^0\right) U\,|\,0\,\rangle, \end{aligned} \tag{2.11}$$

where

$$iA(\boldsymbol{x}) = \langle\, 0 \,|\, U(\boldsymbol{x})^\dagger dU(\boldsymbol{x}) \,|\, 0 \,\rangle. \tag{2.12}$$

In components, we obtain $\psi^0 \to d\psi^0 + iA\psi^0$ as the covariant exterior derivative on the line bundle with a $U(1)$ gauge potential $A$. In the case that the tachyon potential has the form (2.8), this gauge field is also confined to the region $M \subset \mathbb{R}^3$ because of the delta function distribution. In this case, Eq. (2.12) has components only along $M$ (for the proof, see Ref. [26]). If $U(\boldsymbol{x})$ is not globally defined and there are two different diagonalizations $\{U_I(\boldsymbol{x})\}$ at a point, then two gauge potentials of the form (2.12) are related by the $U(1)$ transition function.

This gauge potential should possess a non-trivial $U(1)$-flux

$$iF(\boldsymbol{x}) = idA(\boldsymbol{x}) = \langle\, 0 \,|\, dU(\boldsymbol{x})^\dagger dU(\boldsymbol{x}) \,|\, 0 \,\rangle \tag{2.13}$$

in our setting. Note that the D0-brane charge $k$ for the original $k$ D0-brane system described by $\Phi$ should be maintained as a magnetic flux of charge $k$ in the D2-brane on $M$. We will see this explicitly in the next section.

Note that the induced gauge potential $A$ in Eq. (2.12) can also be seen as a Berry connection, if we regard the base space $\mathbb{R}^3$ as a parameter space of the single Chan–Paton space $\mathbb{C}^N$. This viewpoint appears in Refs. [24,25] in the context of tachyon condensation, and in Ref. [17] in the coherent state method.

## 3. Examples for NC D2-branes

The $k$ D0-brane solution with fluctuation is given by Eq. (2.1):

$$T(\boldsymbol{x}) = u\boldsymbol{\sigma}\cdot(\boldsymbol{x}-\Phi) = u\begin{pmatrix} x^3-\Phi^3 & \bar{z}-\bar{\Phi} \\ z-\Phi & -x^3+\Phi^3 \end{pmatrix}, \tag{3.1}$$

where $z = x^1 + ix^2$ and $\Phi = \Phi^1 + i\Phi^2$. Note that $x^i$ should be understood as $x^i \otimes \mathbf{1}_k$ more precisely. $\Phi^i$ $(i = 1, 2, 3)$ are transverse scalar fields on $k$ D0-branes and are $k \times k$ Hermitian matrices. In this section, we consider examples in which matrices $\Phi^i$ represent NC D2-branes, on a Moyal plane and a fuzzy sphere. The shapes of these branes are commutative $\mathbb{R}^2$ and $S^2$, respectively.

### *3.1. Moyal plane*

An NC D2-brane on the Moyal plane can be made out of $k$ D0-branes, if the scalar field has the profile

$$\Phi^1 = \hat{x}^1, \quad \Phi^2 = \hat{x}^2, \quad \Phi^3 = 0, \tag{3.2}$$

where $\hat{x}^1$ and $\hat{x}^2$ are coordinates on a Moyal plane satisfying $[\hat{x}^1, \hat{x}^2] = i\theta$. By defining the creation/annihilation operators by

$$\hat{a} = \frac{1}{\sqrt{2\theta}}(\hat{x}^1 + i\hat{x}^2), \quad \hat{a}^\dagger = \frac{1}{\sqrt{2\theta}}(\hat{x}^1 - i\hat{x}^2), \tag{3.3}$$

the scalar fields (3.2) are rewritten in complex notation as

$$\Phi = \Phi^1 + i\Phi^2 = \sqrt{2\theta}\hat{a}, \quad \Phi^3 = 0. \tag{3.4}$$

In order to realize them, it is necessary to take $k \to \infty$ and replace matrices $\Phi^i$ with operators acting on the Hilbert space $\ell^2(\mathbb{N})$.

By inserting Eq. (3.2) into Eq. (3.1), the tachyon profile becomes

$$T(\boldsymbol{x}) = u\boldsymbol{\sigma}\cdot(\boldsymbol{x}-\Phi) = u\begin{pmatrix} x^3 & \bar{z}-\sqrt{2\theta}\hat{a}^\dagger \\ z-\sqrt{2\theta}\hat{a} & -x^3 \end{pmatrix}. \tag{3.5}$$

It acts on the Chan–Paton bundle with typical fiber to be the Hilbert space $\mathcal{H} = \ell^2(\mathbb{N})\otimes\mathbb{C}^2$. Let $\{|\, n,\epsilon\,\rangle\,|n = 0,1,2,\ldots,\epsilon = \pm\}$ be its ONB, where $n$ and $\epsilon$ denote the eigenstate for the number operator $\hat{N} = \hat{a}^\dagger\hat{a}$ and the eigenvalues of the Pauli matrix $\sigma_3$, respectively. That is, two component vectors

$$|\, n,+\,\rangle = \begin{pmatrix} |\, n\,\rangle \\ 0 \end{pmatrix}, \quad |\, n,-\,\rangle = \begin{pmatrix} 0 \\ |\, n\,\rangle \end{pmatrix} \tag{3.6}$$

give the basis of $\mathcal{H}$, where $|\, n\,\rangle$ is the ONB of $\ell^2(\mathbb{N})$.

### *3.1.1. Condensation*

We will now study the tachyon condensation of this profile (3.5). To this end, we use the displacement operator for $\alpha \in \mathbb{C}$,

$$D(\alpha) = e^{\alpha\hat{a}^\dagger - \bar{\alpha}\hat{a}} = e^{-|\alpha|^2/2}e^{\alpha\hat{a}^\dagger}e^{-\bar{\alpha}\hat{a}}, \tag{3.7}$$

which is a unitary operator and defines a coherent state $|\,\alpha\,\rangle = D(\alpha)\,|\,0\,\rangle$ [33]. The basic properties are

$$D(\alpha)\hat{a}D(\alpha)^\dagger = \hat{a}-\alpha, \;\; D(\alpha)\hat{a}^\dagger D(\alpha)^\dagger = \hat{a}^\dagger - \bar{\alpha}. \tag{3.8}$$

By using these properties, the $z$-dependence in Eq. (3.5) is extracted as

$$T(\boldsymbol{x}) = uU(z)\begin{pmatrix} x^3 & -\sqrt{2\theta}\hat{a}^\dagger \\ -\sqrt{2\theta}\hat{a} & -x^3 \end{pmatrix}U^\dagger(z), \tag{3.9}$$

where the unitary operator $U(z)$ is given by

$$U(z) = \begin{pmatrix} D(\alpha) & 0 \\ 0 & D(\alpha) \end{pmatrix}, \quad \alpha = \frac{z}{\sqrt{2\theta}}. \tag{3.10}$$

Under the tachyon condensation $u \to \infty$, the surviving mode under the condensation is zero eigenstates of $T^2(\boldsymbol{x})$:

$$T^2(\boldsymbol{x}) = u^2U(z)\begin{pmatrix} (x^3)^2+2\theta\hat{N} & 0 \\ 0 & (x^3)^2+2\theta(\hat{N}+1) \end{pmatrix}U(z)^\dagger. \tag{3.11}$$

It exists only for $x^3 = 0$. Since $\hat{N}$ has the spectrum $\{n = 0,1,2,\ldots\}$, $T^2(\boldsymbol{x})$ has a zero mode of the form

$$U(z)\,|\,0,+\,\rangle = \begin{pmatrix} D(\alpha)\,|\,0\,\rangle \\ 0 \end{pmatrix} \tag{3.12}$$

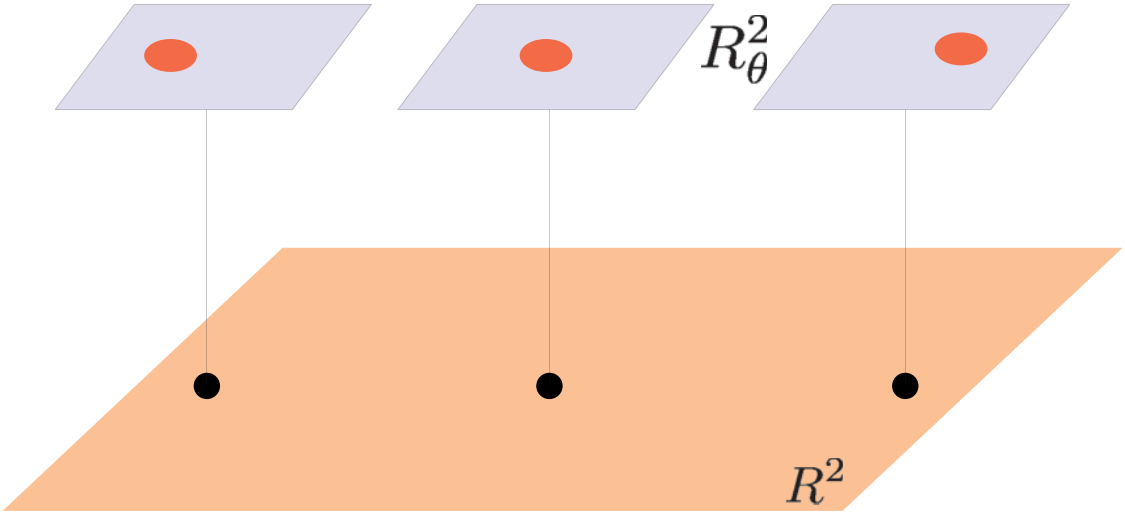


**Fig. 1.** The large plane represents the base space $M = \mathbb{R}^2$. After tachyon condensation, at each point on the base space, we have $D(\alpha)\,|\,0\,\rangle$ as the fiber of the line bundle on $M$. The wave packets of $D(\alpha)\,|\,0\,\rangle$, which have area $2\pi\theta$, are schematically drawn as colored blobs on the smaller planes.

at each point with arbitrary $z = x^1 + ix^2$ and $x^3 = 0$. The tachyon potential reduces to the projection operator onto this zero mode:

$$e^{-T^2} \xrightarrow{u\to\infty} \frac{u}{\sqrt{\pi}}\delta(x^3)P(z), \quad P(z) = U(z)\begin{pmatrix} |\,0\,\rangle\langle\,0\,| & 0 \\ 0 & 0 \end{pmatrix}U(z)^\dagger. \tag{3.13}$$

Here we have used the fact $e^{-u^2(x^3)^2} \to \frac{u}{\sqrt{\pi}}\delta(x^3)$ in the limit $u \to \infty$.

From the delta function, we see that the remnant of this condensation is the real 2D surface $M = \mathbb{R}^2 = \mathbb{C}$, which is considered as a spatial worldvolume of a D2-brane. We emphasize that the obtained worldvolume parameterized by $z$ and $\bar{z}$ is commutative, although we start with a Moyal plane configuration. On the other hand, the projection operator $P(z)$ of the Chan–Paton bundle picks up a coherent state $D(\alpha)\,|\,0\,\rangle$ at each point $z$ on $M$. Because it is 1D subspace at each fiber, the Chan–Paton bundle reduces to a line bundle on $M$. This means a single D2-brane with the gauge group $U(1)$. Moreover, because the fiber $D(\alpha)\,|\,0\,\rangle$ smoothly depends on the base space (recall Eq. (3.10)), this line bundle is non-trivial. This information is encoded in the unitary operator $U(z)$, and we see a further consequence on the gauge flux in the following.

It is worth emphasizing that this result is completely different from the perturbative picture of multiple D0-branes, where a D0-brane is sitting at the origin but fluctuates around the origin in the "directions" of the non-commuting scalar fields $\Phi$, i.e., a single Moyal plane. In our picture, matrices $\Phi$ originally give a family of Moyal planes on $\mathbb{R}^3$ as a Chan–Paton bundle of the non-BPS D3-branes, which, however, reduces to a line bundle on $M = \mathbb{R}^2$ by the tachyon condensation. A schematic picture is given in Fig. 1.

### *3.1.2. Eigenstates*

For completeness, we here diagonalize Eq. (3.5). We give the solution for the eigenvalue problem

$$T(\boldsymbol{x})\,\big|\,\psi_{n,\epsilon}(\boldsymbol{x})\,\big\rangle = t_{n,\epsilon}(\boldsymbol{x})\,\big|\,\psi_{n,\epsilon}(\boldsymbol{x})\,\big\rangle. \tag{3.14}$$

Note that states of the form $D(\alpha)\,|\,n,\epsilon\,\rangle$ give an ONB, since the displacement operator is a unitary operator. Acting $T$ on these states, it is easy to recognize that $D(\alpha)\,|\,0,+\,\rangle$ is already an eigenstate $TD(\alpha)\,|\,0,+\,\rangle = ux^3 D(\alpha)\,|\,0,+\,\rangle$. Thus we write it as $\left|\,\psi_{0,+}\,\right\rangle = D(\alpha)\,|\,0,+\,\rangle$ with $t_{0,+}(\boldsymbol{x}) = ux^3$. Next, for a fixed $n$ ($n \geq 1$), two states $D(\alpha)\,|\,n,+\,\rangle$ and $D(\alpha)\,|\,n-1,+\,\rangle$ form a doublet under $T$, since

$$\begin{aligned} T(\boldsymbol{x})D(\alpha)\,|\,n,+\,\rangle &= uD(\alpha)\left(x^3\,|\,n,+\,\rangle - \sqrt{2\theta n}\,|\,n-1,-\,\rangle\right), \\ T(\boldsymbol{x})D(\alpha)\,|\,n-1,-\,\rangle &= uD(\alpha)\left(-x^3\,|\,n-1,-\,\rangle - \sqrt{2\theta n}\,|\,n,+\,\rangle\right). \end{aligned} \tag{3.15}$$

On this doublet, $T$ is effectively a matrix for each $n$,

$$T^{(n)} = \begin{pmatrix} x^3 & -\sqrt{2\theta n} \\ -\sqrt{2\theta n} & -x^3 \end{pmatrix} = x^3\sigma_3 - \sqrt{2\theta n}\sigma_1, \tag{3.16}$$

which is easily diagonalized by the unitary matrix

$$W^{(n)} = \frac{1}{\sqrt{2|T^{(n)}|(|T^{(n)}| + x^3)}} \begin{pmatrix} |T^{(n)}| + x^3 & \sqrt{2\theta n} \\ -\sqrt{2\theta n} & |T^{(n)}| + x^3 \end{pmatrix}, \tag{3.17}$$

where $|T^{(n)}| = \sqrt{(x^3)^2 + 2\theta n}$. The eigenvalues are $t_{n,\epsilon}(\boldsymbol{x}) = u\epsilon|T^{(n)}|$ and the corresponding eigenstates are

$$\begin{aligned} \left|\,\psi_{n,+}\,\right\rangle &= W^{(n)}_{++}D(\alpha)\,|\,n,+\,\rangle + W^{(n)}_{+-}D(\alpha)\,|\,n-1,-\,\rangle, \\ \left|\,\psi_{n,-}\,\right\rangle &= W^{(n)}_{-+}D(\alpha)\,|\,n,+\,\rangle + W^{(n)}_{--}D(\alpha)\,|\,n-1,-\,\rangle. \end{aligned} \tag{3.18}$$

We can express all the eigenstates as $\left|\,\psi_{n,\epsilon}\,\right\rangle = WD(\alpha)\,|\,n,\epsilon\,\rangle$, by defining $W$ as 1 on $|\,0,+\,\rangle$ and $W^{(n)}$ on the doublet at $n$ as above. These states are orthonormal $\left\langle\,\psi_{n,\epsilon}\,\middle|\,\psi_{n',\epsilon'}\,\right\rangle = \delta_{nn'}\delta_{\epsilon\epsilon'}$, since $W^\dagger W = 1$.

In summary, the set of eigenstates consists of a ground state (singlet) $\left|\,\psi_{0,+}\,\right\rangle = D(\alpha)\,|\,0,+\,\rangle$ with its eigenvalue $t_{0,+}(\boldsymbol{x}) = ux^3$, and the family of doublets $\left|\,\psi_{n,\epsilon}\,\right\rangle$ ($n \geq 1$) with eigenvalues $t_{n,\epsilon}(\boldsymbol{x}) = u\epsilon\sqrt{(x^3)^2 + 2\theta n}$. Under the tachyon condensation, all the doublets are annihilated, because $t_{n,\epsilon}(\boldsymbol{x}) \neq 0$ for all $\boldsymbol{x}$, while the singlet survives on the plane $x^3 = 0$ as states in Eq. (3.12). Note that the mixing between states $|\,n\,\rangle$ and $|\,\pm\,\rangle$ is inevitable. This structure cannot be seen by the part $|\,n\,\rangle$ only (i.e., Chan–Paton space for D0-branes).

### 3.1.3. *Gauge flux*

The tachyon potential (3.13) defines the projective module or equivalently a complex line bundle over $M = \mathbb{R}^2$. The corresponding $U(1)$ gauge connection is given by the Grassmannian connection according to Eq. (2.12). In the present case, the $U(1)$ gauge field on $M = \mathbb{R}^2$ is given by

$$iA(z,\bar{z}) = \langle\,0,+\,|\,U^\dagger(z)dU(z)\,|\,0,+\,\rangle = \langle\,0\,|\,D^\dagger(\alpha)dD(\alpha)\,|\,0\,\rangle. \tag{3.19}$$

After some calculations, we find

$$A = -\frac{i}{4\theta}(\bar{z}dz - zd\bar{z}) = \frac{1}{2\theta}(x^1dx^2 - x^2dx^1) \tag{3.20}$$

(see Appendix A.1 for the derivation). The corresponding field strength on $M$ is given by

$$F = dA = \frac{i}{2\theta}dz \wedge d\bar{z} = \frac{1}{\theta}dx^1 \wedge dx^2. \tag{3.21}$$

A uniform magnetic flux on a D2-brane is interpreted as the D0-brane charge density, and its presence indicates that the resulting system is a bound state of D2 and D0-branes, where D0-branes are dissolved into a D2-brane. In fact, in the Chern–Simons term for a D2-brane, the coupling to the RR 1-form is

$$\frac{1}{2\pi}\int_{\mathbb{R}^2} F = \frac{\mathrm{Vol}(\mathbb{R}^2)}{2\pi\theta}. \tag{3.22}$$

This says that there is a dissolved D0-brane per unit volume $2\pi\theta$. Therefore, the original information on a Moyal plane is converted to a commutative plane with a uniform magnetic flux.

This equivalence between commutative and non-commutative descriptions of the D2–D0 bound states is first shown in Refs. [34,35], in terms of boundary states. We here reproduce the same result within the effective theory on non-BPS D3-branes, but the equivalence is realized in a more direct way. That is, once the D2–D0 bound states are represented in the tachyon profile, the equivalence is realized by the unitary transformation that diagonalizes the tachyon profile.

### 3.2. *Fuzzy sphere*

An NC D2-brane on a fuzzy sphere can be made out of $k$ D0-branes, if the scalar field has the profile

$$\Phi^i = \rho L_i, \qquad [L_i, L_j] = i\varepsilon_{ij}{}^k L_k, \tag{3.23}$$

where $\rho$ is a real parameter and $L_i$ $(i = 1,2,3)$ are $su(2)$ generators in the spin-$\ell$ irreducible representation [36]. Thus it is possible for $k \geq 2$. We denote corresponding $k = 2\ell+1$ states as $|\, m\,\rangle$ $(m = -\ell, -\ell+1, \ldots, \ell-1, \ell)$. Because $\Phi^2 = \rho^2 \boldsymbol{L}^2 = \rho^2 \ell(\ell+1)\mathbf{1}_k = \rho^2 \frac{k^2-1}{4}\mathbf{1}_k$, a naive guess of the radius of this fuzzy sphere is $\rho\sqrt{\frac{k^2-1}{4}}$. We will compare it with the radius of $S^2$ obtained from the tachyon condensation below.

By inserting Eq. (3.23) into Eq. (3.1), the tachyon profile becomes

$$T(\boldsymbol{x}) = u\boldsymbol{\sigma}\cdot(\boldsymbol{x} - \rho\boldsymbol{L}), \tag{3.24}$$

and its square leads to

$$T^2(\boldsymbol{x}) = u^2\left(|\boldsymbol{x}|^2 + \rho^2\boldsymbol{L}^2 - 2\rho(\boldsymbol{x}\cdot\boldsymbol{L}) - \rho^2(\boldsymbol{\sigma}\cdot\boldsymbol{L})\right). \tag{3.25}$$

Here, the ONB of the Chan–Paton Hilbert space $\mathcal{H} = \mathbb{C}^k \otimes \mathbb{C}^2$ is given by $\{|\, m, \epsilon\,\rangle \,|m = -\ell, \ldots, \ell, \epsilon = \pm\}$.

#### 3.2.1. *Condensation*

Here we study the tachyon condensation by diagonalizing $T$ in Eq. (3.24). To this end, we examine the two terms in Eq. (3.24) separately in detail.

a) The term $\boldsymbol{\sigma}\cdot\boldsymbol{x}$ in Eq. (3.24) is independent of the choice of $\Phi$, and it can be diagonalized only patch-wise [26].
First at the origin $\boldsymbol{x} = 0$ in $\mathbb{R}^3$, this term does not contribute to $T$ and is already diagonal. We then divide $\mathbb{R}^3$ except $\boldsymbol{x} = 0$ into two regions:

$$\begin{aligned}\mathcal{U}_N &= \{\boldsymbol{x}\in\mathbb{R}^3 \mid |\boldsymbol{x}| + x^3 \neq 0\} = \{(r,\theta,\varphi)\in\mathbb{R}^3 \mid r\neq 0, \theta\neq\pi\},\\ \mathcal{U}_S &= \{\boldsymbol{x}\in\mathbb{R}^3 \mid |\boldsymbol{x}| - x^3 \neq 0\} = \{(r,\theta,\varphi)\in\mathbb{R}^3 \mid r\neq 0, \theta\neq 0\},\end{aligned} \tag{3.26}$$

where $\boldsymbol{x} = (x^1, x^2, x^3)$ and in the second expression the standard polar coordinates are used. Thus, $\mathcal{U}_N$ is $\mathbb{R}^3$ except for the negative $x^3$-axis, while $\mathcal{U}_S$ is $\mathbb{R}^3$ except for the positive $x^3$-axis. In each region $\mathcal{U}_N$ and $\mathcal{U}_S$, $\boldsymbol{\sigma}\cdot\boldsymbol{x}$ is diagonalized as

$$R^{\dagger}_{N/S}(\Omega)(\boldsymbol{\sigma}\cdot\boldsymbol{x})R_{N/S}(\Omega) = |\boldsymbol{x}|\sigma_3 \tag{3.27}$$

by the corresponding unitary matrix-valued function on $\mathbb{R}^3$:

$$\begin{aligned} R_N(\Omega) &= \frac{1}{\sqrt{2|\boldsymbol{x}|(|\boldsymbol{x}|+x^3)}}\begin{pmatrix} |\boldsymbol{x}|+x^3 & -\bar{z} \\ z & |\boldsymbol{x}|+x^3 \end{pmatrix}, \\ R_S(\Omega) &= \frac{1}{\sqrt{2|\boldsymbol{x}|(|\boldsymbol{x}|-x^3)}}\begin{pmatrix} \bar{z} & -|\boldsymbol{x}|+x^3 \\ |\boldsymbol{x}|-x^3 & z \end{pmatrix}. \end{aligned} \tag{3.28}$$

They depend only on the angular coordinates $\Omega = (\theta, \varphi)$ and are written in polar coordinates as

$$R_N(\Omega) = \begin{pmatrix} \cos\frac{\theta}{2} & -\sin\frac{\theta}{2}e^{-i\varphi} \\ \sin\frac{\theta}{2}e^{i\varphi} & \cos\frac{\theta}{2} \end{pmatrix}, \quad R_S(\Omega) = \begin{pmatrix} \cos\frac{\theta}{2}e^{-i\varphi} & -\sin\frac{\theta}{2} \\ \sin\frac{\theta}{2} & \cos\frac{\theta}{2}e^{i\varphi} \end{pmatrix}. \tag{3.29}$$

The expression $R_N$ in Eq. (3.29) is familiar in quantum mechanics with the diagonalization of a spin with respect to the direction $\hat{\boldsymbol{x}} = \frac{\boldsymbol{x}}{|\boldsymbol{x}|}$, if $S_i = \frac{\sigma_i}{2}$ is considered as the spin-$\frac{1}{2}$ representation. But note that the diagonalization by $R_N$ is ill defined at the south pole $\theta = \pi$.[3] In order to cover all directions, we need another open set $\mathcal{U}_S$.

b) The term $\boldsymbol{\sigma}\cdot\boldsymbol{L}$ in Eq. (3.24) or, more properly, the term $\boldsymbol{S}\cdot\boldsymbol{L}$, is similar to the spin–orbit interaction in quantum mechanics. Thus, under the total spin $\boldsymbol{J} = \boldsymbol{L} + \boldsymbol{S}$, the tensor product representation $[\ell]\otimes[\frac{1}{2}]$ decomposes into two irreducible representations $[\ell+\frac{1}{2}]\oplus[\ell-\frac{1}{2}]$. Since $\boldsymbol{J}^2 = \boldsymbol{L}^2 + \boldsymbol{S}^2 + 2(\boldsymbol{S}\cdot\boldsymbol{L})$, the operator $\boldsymbol{\sigma}\cdot\boldsymbol{L}$ has the eigenvalue $\ell$ in all states in $[\ell+\frac{1}{2}]$, and the eigenvalue $-(\ell+1)$ in all states in $[\ell-\frac{1}{2}]$. This shows that two kinds of states should be mixed in order to diagonalize $\boldsymbol{\sigma}\cdot\boldsymbol{L}$. The ONB ($2\ell+2$ states) of $[\ell+\frac{1}{2}]$ is given by eigenstates of $J_3$ as

$$\left|\, m+\tfrac{1}{2}\,\right\rangle_{\ell+\frac{1}{2}} = \alpha_m \,|\, m,+\,\rangle + \beta_m \,|\, m+1,-\,\rangle, \tag{3.30}$$

where $m = -\ell-1, -\ell, \ldots, \ell$, and

$$\alpha_m = \sqrt{\frac{\ell+m+1}{2\ell+1}}, \qquad \beta_m = \sqrt{\frac{\ell-m}{2\ell+1}}. \tag{3.31}$$

Note that two particular states,

$$\left|\, \ell+\tfrac{1}{2}\,\right\rangle_{\ell+\frac{1}{2}} = |\,\ell,+\,\rangle, \quad \left|\, -\ell-\tfrac{1}{2}\,\right\rangle_{\ell+\frac{1}{2}} = |\,-\ell,-\,\rangle, \tag{3.32}$$

exist in this representation. On the other hand, the ONB ($2\ell$ states) of $[\ell-\frac{1}{2}]$ is

$$\left|\, m+\tfrac{1}{2}\,\right\rangle_{\ell-\frac{1}{2}} = \beta_m \,|\, m,+\,\rangle - \alpha_m \,|\, m+1,-\,\rangle, \tag{3.33}$$

where $m = -\ell, -\ell+1, \ldots, \ell-1$.

In order to diagonalize $T$ in Eq. (3.24), we have to consider both aspects of a) and b) simultaneously; i.e., we have to consider the total spin b) in a patch-wise way a).

[3] It is obvious in Eq. (3.28) if $|\boldsymbol{x}| + x^3 = 0$, and in Eq. (3.29) it is ill defined because $\varphi$ is undefined at $\theta = \pi$.

### 3.2.2. *Condensation in $\mathcal{U}_N$*

First, we consider points in the open set $\mathcal{U}_N$. As stated, $R_N$ in a) appears in the spin along the axis through $\boldsymbol{x}$. In general, for an angular momentum operator $\boldsymbol{J}$, the term $\boldsymbol{x}\cdot\boldsymbol{J}$ determines the new "north pole" direction through $\boldsymbol{x}$. Then eigenvalues of $J_3' = \hat{\boldsymbol{x}}\cdot\boldsymbol{J}$ can also be used to label the ONB. Here $J_i$ and $J_3'$ are related by an $SO(3)$ rotation $\Lambda_j^i$ that sends the unit vector through the point $\Omega = (\theta,\varphi)$ on the unit sphere to that pointing to the north pole $\boldsymbol{x} = (0,0,1)$. This rotation is generated by the unitary operator,

$$\begin{aligned} R_N(\Omega) &= e^{-i\varphi J_3} e^{-i\theta J_2} e^{i\varphi J_3} \\ &= e^{-\frac{1}{2}\theta(e^{-i\varphi}J_+ - e^{i\varphi}J_-)}, \end{aligned} \tag{3.34}$$

which satisfies

$$R_N^\dagger(\Omega) J_i R_N(\Omega) = \Lambda_i^j J_j, \tag{3.35}$$

with

$$\Lambda = \begin{pmatrix} \cos\varphi & -\sin\varphi & 0 \\ \sin\varphi & \cos\varphi & 0 \\ 0 & 0 & 1 \end{pmatrix} \begin{pmatrix} \cos\theta & 0 & \sin\theta \\ 0 & 1 & 0 \\ -\sin\theta & 0 & \cos\theta \end{pmatrix} \begin{pmatrix} \cos\varphi & \sin\varphi & 0 \\ -\sin\varphi & \cos\varphi & 0 \\ 0 & 0 & 1 \end{pmatrix} \tag{3.36}$$

(see Appendix A.2 for a proof). The previous $R_N$ in Eq. (3.29) is the spin-1/2 case of Eq. (3.34). This implies the spin-$j$ analogue of Eq. (3.27):

$$R_N^\dagger(\Omega)(\boldsymbol{x}\cdot\boldsymbol{J}) R_N(\Omega) = |\boldsymbol{x}| J_3. \tag{3.37}$$

In particular, the transformed state $R_N(\Omega)\,|\,j\,\rangle$ of the highest weight state $|\,j\,\rangle$ is called the Bloch (spin) coherent state [33].

In our case, consider Eq. (3.34) for the total spin $\boldsymbol{J} = \boldsymbol{L} + \boldsymbol{S}$. We can then split it as $R_N(\Omega) = R_N^{(L)}(\Omega) R_N^{(S)}(\Omega)$, with Eq. (3.34) for $\boldsymbol{S}$ and $\boldsymbol{L}$, respectively. For the tachyon profile (3.24), it is obvious that this operator still diagonalizes $\boldsymbol{x}\cdot\boldsymbol{\sigma} = 2\boldsymbol{x}\cdot\boldsymbol{S}$. On the other hand, it keeps $\boldsymbol{\sigma}\cdot\boldsymbol{L} = 2\boldsymbol{S}\cdot\boldsymbol{L}$ invariant, since it is an $SO(3)$ scalar operator. Therefore, the tachyon profile is written as

$$T(\boldsymbol{x}) = u R_N(\Omega)(|\boldsymbol{x}|\sigma_3 - \rho\boldsymbol{\sigma}\cdot\boldsymbol{L}) R_N^\dagger(\Omega). \tag{3.38}$$

Note that the $\Omega$=$(\theta,\varphi)$-dependence is absorbed into $R_N(\Omega)$. It is then reasonable to use the orthonormal basis of the form $R_N(\Omega)\,|\,m,\epsilon\,\rangle$ to find the eigenstates of $T$. According to b), the second term $\boldsymbol{\sigma}\cdot\boldsymbol{L}$ in Eq. (3.38) is diagonalized by the states of the form $R_N(\Omega)\,\big|\,m+\frac{1}{2}\big\rangle_{\ell\pm\frac{1}{2}}$, but we should also take into account the first term. It turns out that two particular states $R_N(\Omega)\,|\,\ell,+\,\rangle$ and $R_N(\Omega)\,|\,-\ell,-\,\rangle$ are already the eigenstates of $T$. By using

$$\boldsymbol{\sigma}\cdot\boldsymbol{L} = \sigma_3 L_3 + \tfrac{1}{2}(\sigma_+ L_- + \sigma_- L_+), \tag{3.39}$$

we obtain

$$\begin{aligned} T R_N(\Omega)\,|\,\ell,+\,\rangle &= u R_N(\Omega)\left\{(|\boldsymbol{x}| - \rho L_3)\sigma_3 - \tfrac{\rho}{2}(\sigma_+ L_- + \sigma_- L_+)\right\}|\,\ell,+\,\rangle \\ &= u(|\boldsymbol{x}| - \rho\ell) R_N(\Omega)\,|\,\ell,+\,\rangle, \end{aligned} \tag{3.40}$$

which is zero at a point in $\mathcal{U}_N$ with $|\boldsymbol{x}| = \rho\ell$. Thus, a sphere with radius $\rho\ell$ survives under the tachyon condensation. Similarly, we have

$$\begin{aligned} TR_N(\Omega)\,|-\ell,-\rangle &= uR_N(\Omega)\left\{(|\boldsymbol{x}|-\rho L_3)\sigma_3 - \tfrac{\rho}{2}(\sigma_+L_- + \sigma_-L_+)\right\}|-\ell,-\rangle \\ &= -u(|\boldsymbol{x}|+\rho\ell)R_N(\Omega)\,|-\ell,-\rangle, \end{aligned} \tag{3.41}$$

which is always negative (no zero locus); thus, this state is completely annihilated under the tachyon condensation.

For the remaining eigenstates, consider a 2D subspace of the form

$$R_N(\Omega)\,\{a_m\,|\,m,+\rangle + b_m\,|\,m+1,-\rangle\} \quad \leftrightarrow \begin{pmatrix} a_m \\ b_m \end{pmatrix} \tag{3.42}$$

for a fixed $m$ with $m = -\ell, -\ell+1, \ldots, \ell-1$ and with arbitrary coefficients $a_m(\boldsymbol{x})$ and $b_m(\boldsymbol{x})$. The point is that $T(\boldsymbol{x})$ is closed within this subspace:

$$\begin{aligned} TR_N(\Omega)\,|\,m,+\rangle &= uR_N(\Omega)\left\{(|\boldsymbol{x}|-\rho L_3)\sigma_3 - \tfrac{\rho}{2}(\sigma_+L_- + \sigma_-L_+)\right\}|\,m,+\rangle \\ &= uR_N(\Omega)\left\{(|\boldsymbol{x}|-\rho m)\,|\,m,+\rangle - \rho\sqrt{(\ell-m)(\ell+m+1)}\,|\,m+1,-\rangle\right\}, \\ TR_N(\Omega)\,|\,m+1,-\rangle &= uR_N(\Omega)\left\{(|\boldsymbol{x}|-\rho L_3)\sigma_3 - \tfrac{\rho}{2}(\sigma_+L_- + \sigma_-L_+)\right\}|\,m+1,-\rangle \\ &= uR_N(\Omega)\left\{-(|\boldsymbol{x}|-\rho(m+1))\,|\,m+1,-\rangle - \rho\sqrt{(\ell+m+1)(\ell-m)}\,|\,m,+\rangle\right\}. \end{aligned} \tag{3.43}$$

This implies $T(\boldsymbol{x})$ is effectively represented as a $2\times 2$ matrix-valued function $T^{(m)}(|\boldsymbol{x}|)$ for each $m$:

$$T^{(m)}\begin{pmatrix} a_m \\ b_m \end{pmatrix} = u\begin{pmatrix} |\boldsymbol{x}|-\rho m & -\rho\sqrt{(\ell-m)(\ell+m+1)} \\ -\rho\sqrt{(\ell-m)(\ell+m+1)} & -|\boldsymbol{x}|+\rho(m+1) \end{pmatrix}\begin{pmatrix} a_m \\ b_m \end{pmatrix}. \tag{3.44}$$

This matrix is diagonalized in a standard way (see Appendix A.3 for more details) and the eigenvalues at each point (i.e., functions) are found to be

$$\lambda_\pm^{(m)}(|\boldsymbol{x}|) = u\left[\tfrac{\rho}{2} \pm \left|M^{(m)}\right|\right], \tag{3.45}$$

with

$$\left|M^{(m)}\right| \equiv \sqrt{\rho^2(\ell-m)(\ell+m+1)\left(|\boldsymbol{x}|-\rho(m+\tfrac{1}{2})\right)^2}. \tag{3.46}$$

For all $m = -\ell, -\ell+1, \ldots, \ell-1$, $|M^{(m)}|^2$ satisfies $|M^{(m)}|^2 \geq 2\rho^2\ell$, and thus $|M^{(m)}| > \rho/2$ for all spin $\ell \geq 1/2$. This implies that for any $\ell$ and $m$, two eigenvalues $\lambda_\pm^{(m)}$ are always non-zero at any point $\boldsymbol{x} \in \mathcal{U}_N$. Therefore, the tachyon condensation annihilates the corresponding eigenstates.

In summary, the eigenvalues of $T(\boldsymbol{x})$ and the corresponding eigenstates are given by

$$\begin{aligned} |\boldsymbol{x}| - \rho\ell &: \ R_N(\Omega)\,|\,\ell,+\rangle, \\ -(|\boldsymbol{x}|+\rho\ell) &: \ R_N(\Omega)\,|-\ell,-\rangle, \\ \lambda_+^{(m)}(|\boldsymbol{x}|) &: \ R_N(\Omega)\left\{W_{11}^{(m)}\,|\,m,+\rangle + W_{21}^{(m)}\,|\,m+1,-\rangle\right\}, \\ \lambda_-^{(m)}(|\boldsymbol{x}|) &: \ R_N(\Omega)\left\{W_{12}^{(m)}\,|\,m,+\rangle + W_{22}^{(m)}\,|\,m+1,-\rangle\right\}, \end{aligned} \tag{3.47}$$

where the explicit form of the matrix $W^{(m)}(|\boldsymbol{x}|)$ is given in Appendix A.3. The first state becomes a zero mode at a point $\boldsymbol{x} \in \mathcal{U}_N$ with the radius $|\boldsymbol{x}| = \rho\ell$. The other states always vanish under the tachyon condensation.

### 3.2.3. *Condensation in $\mathcal{U}_S$*

In $\mathcal{U}_S$, the eigenvalues of the tachyon profile are the same as in Eq. (3.47) in $\mathcal{U}_N$, but another unitary operator $R_S$ is needed to diagonalize $T$ and a different state survives under the tachyon condensation. To see this, consider a point on the negative $x^3$-axis, $\boldsymbol{x} = (0, 0, -|\boldsymbol{x}|)$. Because of $\boldsymbol{\sigma} \cdot \boldsymbol{x} = -|\boldsymbol{x}|\sigma_3$ and by using Eq. (3.39), we find

$$\begin{aligned} T(\boldsymbol{x}) \,|\, -\ell, - \,\rangle &= u\,(|\boldsymbol{x}| - \rho\ell) \,|\, -\ell, - \,\rangle, \\ T(\boldsymbol{x}) \,|\, \ell, + \,\rangle &= u\,(-|\boldsymbol{x}| - \rho\ell) \,|\, \ell, + \,\rangle. \end{aligned} \tag{3.48}$$

This shows that the surviving state is the lowest weight state $|\, -\ell, - \,\rangle$ around the south pole, if $|\boldsymbol{x}| = \rho\ell$. This is extended to any point $\boldsymbol{x} = (|\boldsymbol{x}|, \theta, \varphi) \in \mathcal{U}_S$ ($\theta \neq 0$) by sending it to the south pole generated by the unitary operator:

$$\begin{aligned} \tilde{R}_S(\Omega) &= e^{-i\varphi J_3} e^{i(\pi-\theta)\varphi J_2} e^{i\varphi J_3} \\ &= e^{-\frac{1}{2}(\pi-\theta)(e^{-i\varphi}J_+ - e^{i\varphi}J_-)}. \end{aligned} \tag{3.49}$$

Then, the Bloch coherent state $\tilde{R}_S(\Omega) \,|\, -\ell, - \,\rangle$ with respect to the south pole is shown to be an eigenstate of $T(\boldsymbol{x})$:

$$\begin{aligned} T(\boldsymbol{x})\tilde{R}_S(\Omega) \,|\, -\ell, - \,\rangle &= u\tilde{R}_S(\Omega)\,(-|\boldsymbol{x}|\sigma_3 - \rho\boldsymbol{\sigma} \cdot \boldsymbol{L}) \,|\, -\ell, - \,\rangle \\ &= u\,(|\boldsymbol{x}| - \rho\ell)\,\tilde{R}_S(\Omega) \,|\, -\ell, - \,\rangle, \end{aligned} \tag{3.50}$$

which is the zero mode if $|\boldsymbol{x}| = \rho\ell$. Finding the other eigenstates uses a similar procedure.

Although this treatment is sufficient when we are interested only in $\mathcal{U}_S$, it should actually be consistent with the result in $\mathcal{U}_N$ in the overlapping region $\mathcal{U}_{NS} = \mathcal{U}_N \cap \mathcal{U}_S$. The remaining 1D fibers of both constructions should be identified with each other; i.e., the difference should be at most a $U(1)$ phase. To this end, we insert an extra rotation $\Theta = e^{-i\pi J_2}$ on the state in $\mathcal{U}_S$ to diagonalize $T(\boldsymbol{x})$. For $\boldsymbol{J} = \boldsymbol{S}$, it is the Wigner time reversal operator,

$$\Theta^{(S)} = e^{-i\pi\frac{\sigma_2}{2}} = -i\sigma_2 = \begin{pmatrix} 0 & -1 \\ 1 & 0 \end{pmatrix}, \tag{3.51}$$

which flips $|\, + \,\rangle$ and $|\, - \,\rangle$. In general, due to the relations

$$\Theta^\dagger J_{1,3}\Theta = -J_{1,3}, \quad \Theta^\dagger J_2 \Theta = J_2, \tag{3.52}$$

the state $\Theta \,|\, m, \epsilon \,\rangle$ is the eigenstate with an alternating sign:

$$J_3\Theta \,|\, m, \epsilon \,\rangle = -\Theta J_3 \,|\, m, \epsilon \,\rangle = -(m + \epsilon)\Theta \,|\, m, \epsilon \,\rangle. \tag{3.53}$$

By the same relations, we also have

$$\begin{aligned} \Theta^\dagger(\boldsymbol{\sigma} \cdot \boldsymbol{L})\Theta &= \boldsymbol{\sigma} \cdot \boldsymbol{L}, \\ \Theta^\dagger(-|\boldsymbol{x}|\sigma_3)\Theta &= +|\boldsymbol{x}|\sigma_3. \end{aligned} \tag{3.54}$$

We now define[4]

$$R_S(\Omega) = \tilde{R}_S(\Omega)\Theta. \tag{3.55}$$

Then the tachyon profile in $\mathcal{U}_S$ is written as

$$T(\boldsymbol{x}) = uR_S(\Omega)\,(|\boldsymbol{x}|\sigma_3 - \rho\boldsymbol{\sigma}\cdot\boldsymbol{L})\,R_S^\dagger(\Omega). \tag{3.56}$$

Since the term inside the brackets is the same as in $\mathcal{U}_N$, it clearly shows that the eigenvalues of $T$ are the same as $\mathcal{U}_N$ as required, and the corresponding eigenstates are given by

$$\begin{aligned}
|\boldsymbol{x}| - \rho\ell :&\quad R_S(\Omega)\,|\,\ell,+\,\rangle,\\
-(|\boldsymbol{x}| + \rho\ell) :&\quad R_S(\Omega)\,|\,-\ell,-\,\rangle,\\
\lambda_+^{(m)}(|\boldsymbol{x}|) :&\quad R_S(\Omega)\left\{W_{11}^{(m)}\,|\,m,+\,\rangle + W_{21}^{(m)}\,|\,m+1,-\,\rangle\right\},\\
\lambda_-^{(m)}(|\boldsymbol{x}|) :&\quad R_S(\Omega)\left\{W_{12}^{(m)}\,|\,m,+\,\rangle + W_{22}^{(m)}\,|\,m+1,-\,\rangle\right\}.
\end{aligned} \tag{3.57}$$

The first state becomes a zero mode at any point $\boldsymbol{x} \in \mathcal{U}_S$ with the radius $|\boldsymbol{x}| = \rho\ell$. The other states always vanish under the tachyon condensation.

### *3.2.4. Gluing in the overlap $\mathcal{U}_{NS}$*

The zero modes in $\mathcal{U}_N$ and $\mathcal{U}_S$ are now written respectively as $R_N(\Omega)\,|\,\ell,+\,\rangle$ and $R_S(\Omega)\,|\,\ell,+\,\rangle$. In the overlapping region $\mathcal{U}_{NS}$, they are identified up to a $U(1)$ gauge transformation (transition function, more properly).

To see this, it is worth rewriting $R_S(\Omega)$ in Eq. (3.55) as (valid for $\theta \neq 0, \pi$)

$$\begin{aligned}
R_S(\Omega) &= \tilde{R}_S(\Omega)\Theta\\
&= e^{-i\varphi J_3}e^{i(\pi-\theta)J_2}e^{i\varphi J_3}e^{-i\pi J_2}\\
&= (e^{-i\varphi J_3}e^{-i\theta J_2}e^{i\varphi J_3})e^{-2i\varphi J_3}\\
&= R_N(\Omega)e^{-2i\varphi J_3}.
\end{aligned} \tag{3.58}$$

By acting this on the state $|\,m,\epsilon\,\rangle$, it implies

$$R_S(\Omega)\,|\,m,\epsilon\,\rangle = e^{-2i\varphi(m+\frac{\epsilon}{2})}R_N(\Omega)\,|\,m,\epsilon\,\rangle. \tag{3.59}$$

This shows that two states $R_S(\Omega)\,|\,m,\epsilon\,\rangle$ and $R_N(\Omega)\,|\,m,\epsilon\,\rangle$ are related by a $U(1)$ phase for fixed $(m,\epsilon)$. Hence, the transition function is $U(1)^{2k}$-valued:

$$R_N^\dagger(\Omega)R_S(\Omega) = e^{-2i\varphi J_3}. \tag{3.60}$$

In particular, we obtain

$$R_S(\Omega)\,|\,\ell,+\,\rangle = e^{-ik\varphi}R_N(\Omega)\,|\,\ell,+\,\rangle, \tag{3.61}$$

since $2(\ell+\frac{1}{2}) = k$. This is nothing but the $U(1)$ transition function for the Wu–Yang $k$-monopole.

[4] There is an constant phase ambiguity in defining $\Theta$. It can be shown that the spin-1/2 part $R_S^{(S)}$ coincides with $R_S$ in Eq. (3.28) so that our choice of $\Theta$ is to be consistent with Ref. [26].

### 3.2.5. *Structure of the tachyon potential*

Having found the eigenvalues of $T(\boldsymbol{x})$, it is easy to write the tachyon potential in the spectral decomposition. Then, it has the form (2.8) as

$$
\begin{aligned}
&e^{-T^2} \xrightarrow{u\to\infty} \frac{u}{\sqrt{\pi}}\delta(|\boldsymbol{x}| - \rho\ell)P_{N/S}(\Omega),\\
&P_N(\Omega) = R_N(\Omega)\,|\,\ell,+\,\rangle\,\langle\,\ell,+\,|\,R_N^\dagger(\Omega),\\
&P_S(\Omega) = R_S(\Omega)\,|\,\ell,+\,\rangle\,\langle\,\ell,+\,|\,R_S^\dagger(\Omega).
\end{aligned}
\tag{3.62}
$$

Here we have used the fact $e^{-u^2(|\boldsymbol{x}|-\rho\ell)^2} \to \frac{u}{\sqrt{\pi}}\delta(|\boldsymbol{x}| - \rho\ell)$ in the limit $u \to \infty$ on the radial delta function [26].

Matrices $\Phi$ originally give a family of fuzzy spheres on $\mathbb{R}^3$ as a Chan–Paton bundle of non-BPS D3-branes. This potential controls the reduction of both the worldvolume and the Chan–Paton space. The worldvolume $\mathbb{R}^3$ of the non-BPS D3-branes reduces to the sphere $M = S^2$ defined by $|\boldsymbol{x}| = \rho\ell$, which is considered as a spherical D2-brane. This sphere is commutative and embedded in $\mathbb{R}^3$ (thus in the spacetime as well). At each point on the sphere specified by $\Omega = (\theta, \varphi)$, the original Chan–Paton space reduces to a 1D subspace $R_N(\Omega)\,|\,\ell,+\,\rangle$ on $\mathcal{U}_N$ or $R_S(\Omega)\,|\,\ell,+\,\rangle$ on $\mathcal{U}_S$, which are related by a $U(1)$ transition function on $\mathcal{U}_{NS}$. It is essentially the Bloch coherent state. A schematic picture is given in Fig. 2. The projection operators $P_N(\Omega)$ and $P_S(\Omega)$ also define an induced $U(1)$-gauge connection, as we will see.

It is interesting that the obtained radius $\rho\ell$ of $S^2$ is different from the expected "radius" of the fuzzy sphere $\rho\sqrt{\ell(\ell+1)}$. Our result should also be compared with the radius given by the charge density formula [7][5]. The radius can be any value at this stage, because of an arbitrary constant $\rho$. It would be determined by the dynamics of the D2-brane, since $\rho$ is regarded as a constant mode of a transverse scalar field on the spherical D2-brane, as analyzed by [6,26].

### 3.2.6. *Induced gauge connection*

The tachyon potential (3.62) defines the projective module or equivalently a complex line bundle over $M = S^2$. The corresponding $U(1)$ gauge connection (2.12) is given patch-wise; i.e., the gauge potentials $A_N$ on $\mathcal{U}_N$ and $A_S$ on $\mathcal{U}_S$ are given respectively by

$$
\begin{aligned}
iA_N(\Omega) &= \langle\,\ell,+\,|\,R_N^\dagger(\Omega)dR_N(\Omega)\,|\,\ell,+\,\rangle,\\
iA_S(\Omega) &= \langle\,\ell,+\,|\,R_S^\dagger(\Omega)dR_S(\Omega)\,|\,\ell,+\,\rangle.
\end{aligned}
\tag{3.63}
$$

After some algebra, we obtain

$$
\begin{aligned}
A_N(\Omega) &= \tfrac{1}{2}k(1-\cos\theta)d\varphi,\\
A_S(\Omega) &= -\tfrac{1}{2}k(1+\cos\theta)d\varphi,
\end{aligned}
\tag{3.64}
$$

where $k = 2\ell + 1$. On the overlap $\mathcal{U}_{NS}$, they are related by the $U(1)$ transition function $e^{-ik\varphi}$:

$$
A_S = e^{ik\varphi}A_N e^{-ik\varphi} - ie^{ik\varphi}de^{-ik\varphi}. \tag{3.65}
$$

[5] The original charge density is supported on the family of spherical shells at finite $k$, but the author of Ref. [7] argued that the commutator corrections improve the formula to give a single sphere with a physical radius $\rho\sqrt{\ell(\ell+1)}$. Our result supports this improvement but the radii do not coincide with each other.

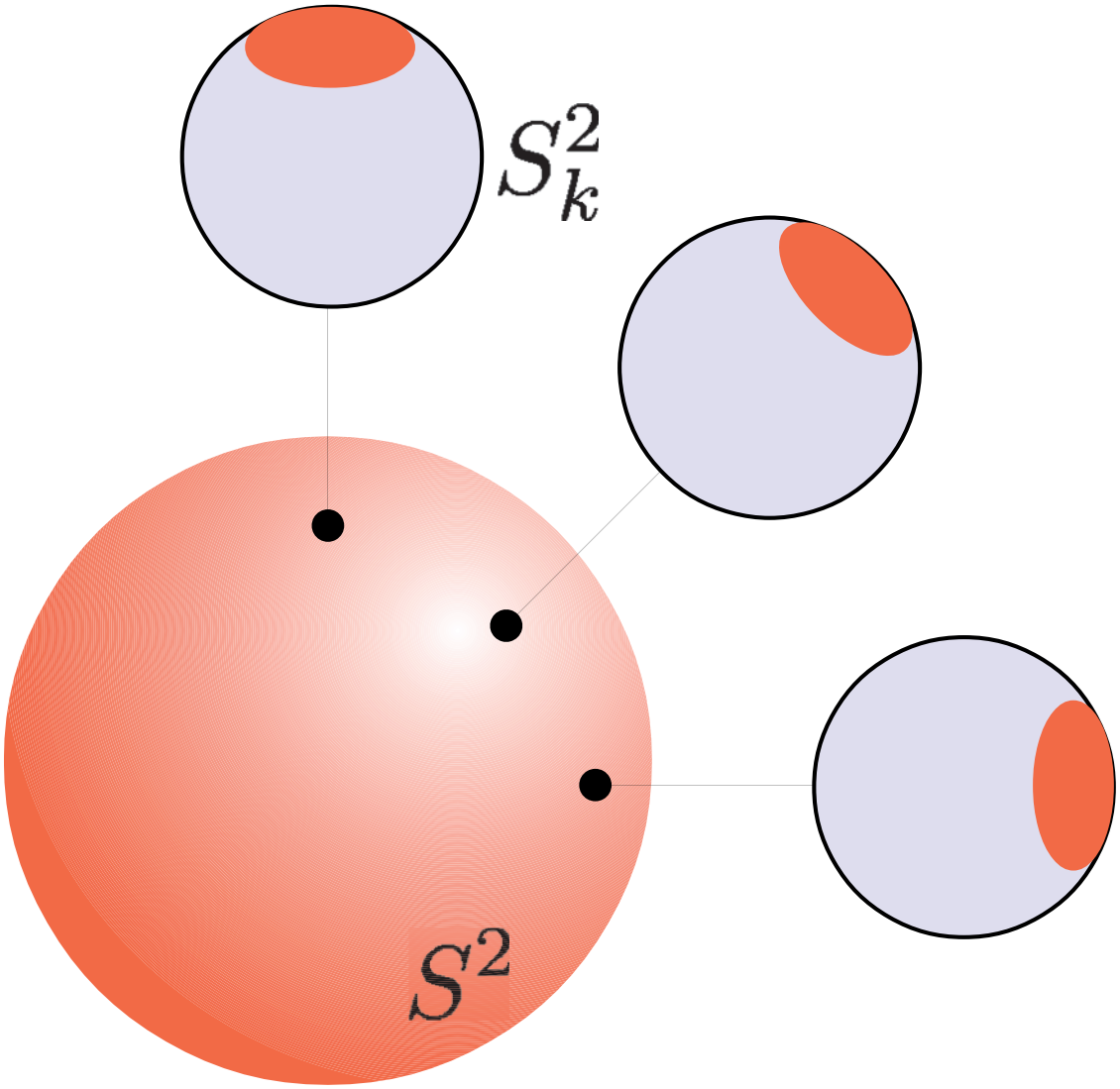


**Fig. 2.** The large sphere represents the base space $M = S^2$, and the small spheres are a family of fuzzy spheres. A fuzzy sphere at the north pole is divided by ring-shaped regions, which correspond to $|\, m, \epsilon \,\rangle$ and its top corresponds to the zero mode $|\, \ell, + \,\rangle$. If we move on the base space $M$ to the point $\Omega$, the fuzzy sphere is divided by regions according to the spin along $\Omega$, with its top being a coherent state $R_N(\Omega)\,|\, \ell, + \,\rangle$.

The $U(1)$ field strength is defined patch-wise by $F|_{\mathcal{U}_N} = dA_N$ and $F|_{\mathcal{U}_S} = dA_S$, but in fact it is globally defined:

$$F = \tfrac{1}{2} k \sin\theta d\theta \wedge d\varphi. \tag{3.66}$$

This configuration is nothing but the Wu–Yang $k$-monopole [37]. The RR-charge originally carried by $k$ D0-branes is maintained by this $U(1)$-flux on a spherical D2-brane, where D0-branes are dissolved into a D2-brane. In fact, in the Chern–Simons term for a D2-brane, the coupling to the RR 1-form is

$$\frac{1}{2\pi}\int_{S^2} F = \frac{k}{4\pi}\int_{S^2} \sin\theta d\theta \wedge d\varphi = k. \tag{3.67}$$

This result is independent of $\rho$.

## 4. Myers term and K-homology

We are considering the problem of mutually non-commuting matrix scalar fields $\Phi$ on multiple D0-branes. The system of $k$ D0-branes with matrix scalar fields $\Phi$ reduces by the tachyon condensation to the region $M$ in the ($\mathbb{R}^3$ part of) spacetime, equipped with a Chan–Paton bundle $E$ over $M$ with $k$-magnetic flux. Thus, we call the region $M$, or a pair $(M, E)$, the shape of the D0-branes. In our simple example above, both $M = \mathbb{R}^2$ and $M = S^2$ are regarded as the worldvolume of a D2-brane and the resulting system $(M, E)$ is identified as a D2–D0 bound state, where $k$ D0-branes are resolved into the D2-brane. This is consistent with the fact that the Myers term produces D2-brane charge density. However, it is not evident if the region $M$ can always be identified as D-branes in more general scalar fields $\Phi$. In this section, we discuss the technical result in the previous section from conceptual grounds, and propose a possible physical interpretation of the shape of multiple D0-branes[6].

The point of our notion of the shape is that it is completely independent of the coordinate interpretation for $\Phi$ and of large $N$. We only use the fact that the zero locus of the tachyon profile gives a defect made out of D0-branes. The underlying belief is that all the D-brane systems are described as solitons by the tachyon condensation and that K-theory classifies all of them [21,22,31]. Therefore, it is natural to understand the meaning of the shape according to this belief, instead of the coordinate interpretation. In the following, we elaborate on the structure of solitons and then propose that the shape fits nicely with classification by K-homology, i.e., the Poincaré dual to K-theory. This says that the shape is classified as a D-brane system. In particular, the Myers term can be incorporated in K-homology.

### 4.1. *Structure of the solitons*

The original ABS construction ($T(\boldsymbol{x})$ in Eq. (2.1) with $\Phi = 0$) represents a ($k$-tuple of) codimension-3 solitons sitting at the origin. It winds the field space $SU(2)$ once around $S^2$ at the asymptotic infinity $|\boldsymbol{x}| \to \infty$ in $\mathbb{R}^3$. Let us first discuss to what extent the addition of the matrix scalar fields $\Phi$ on D0-branes changes the structure of the soliton from the original ABS construction of D0-branes.

One may think that adding scalar fields $\Phi$ in Eq. (2.1) to the tachyon profile does not change this asymptotic structure since it is just a continuous deformation of the ABS solution. This is true for finite $u$ and for finite $k$. However, as we will soon see below, the asymptotic behavior itself can be changed by adding proper $\Phi$ with $k = \infty$. Furthermore, even if $k$ is finite, it may affect the structure of the soliton in the limit of $u \to \infty$. Note that the scalar fields $\Phi$ change the tachyon profile $T(\boldsymbol{x})$ at each point $\boldsymbol{x}$, not just at the origin.

To see this more explicitly, we first recall the Moyal case. After the change of basis as in Eq. (3.9), only the zero eigenfunction $t_{0,+}(\boldsymbol{x}) = ux^3$ contributes to the remaining defect. This zero mode has the form of a codimension-1 kink along the $x^3$-direction. The asymptotic behavior is $t_{0,+}(x^3 = \pm\infty) = \pm\infty$, which is evidently different from the ABS construction before adding $\Phi$. The kink charge is shown to be related to the D2-brane charge $\frac{1}{u\,\mathrm{Vol}(\mathbb{R})}\int dx^3 \partial_3 t_{0,+}(\boldsymbol{x}) = 1$. This drastic change of the asymptotic region is due to the $k \to \infty$ effect.

Next we move to the fuzzy $S^2$ case. In this case, the asymptotic region is unchanged, but the structure at the origin is deformed. After a change of basis, as seen, e.g., in Eq. (3.47), the zero eigenfunction is $t_{\ell,+}(\boldsymbol{x}) = u(|\boldsymbol{x}| - \rho\ell)$. This satisfies the boundary conditions $t_{\ell,+}(|\boldsymbol{x}| = 0) = -u\rho\ell \to -\infty$ and $t_{\ell,+}(|\boldsymbol{x}| = \infty) = \infty$ that relate two different vacua. The limit $u \to \infty$ is important in this situation;

[6] The discussion in this section is mainly based on our answers to S.Terashima's questions. We thank him for this private communication.

it behaves as a kink along the radial direction. This is the same behavior as the spherical D2-brane studied in Ref. [26].

In both cases, since the structure of the soliton is changed, it is no longer a system made of only D0-branes. The appearance of a kink after the deformation is a sign that the defect is actually a D2–D0 bound state. For more general scalar fields $\Phi$, there may appear defects with all possible codimensions $0, 1, 2, 3$. Of course, if we start not with a D3-brane but with non-BPS D9-branes, all nine transverse scalar fields can also be considered as a deformation of codimension-9 ABS construction.

### *4.2. More on the shape of D0-branes*

Although we have considered only two examples, the Moyal plane and the fuzzy sphere, the analysis itself can be applied for more general cases. In general, the shape $M$ of D0-branes is just the zero locus of the tachyon profile for given matrices $\Phi$. Here an important fact is the tachyon field can always be diagonalized for any $\Phi$. Thus, the zero locus $M$ is always determined uniquely.

When all $k \times k$ matrices $\Phi$ are diagonal, then the zero locus $M$ consists of $k$ different points in $\mathbb{R}^3$. This is still true for $k = \infty$. For example, let $\Phi^2 = \hat{x}^1$ and $\Phi^2 = \hat{x}^2$ with commutative $[\hat{x}^1, \hat{x}^2] = 0$ (i.e., $\theta = 0$ in the Moyal case); the shape is then given by the point set $M = \mathbb{R}^2$. We know that this $M$ does not mean a D2-brane (Neumann boundary state along $\mathbb{R}^2$) but infinitely many D0-branes aligned on $\mathbb{R}^2$ (a family of Dirichlet boundary states). Thus, $M$ itself does not see this difference. On the other hand, in the Moyal case, we know that the shape $M = \mathbb{R}^2$ is a D2-brane worldvolume of a D2–D0 bound state, i.e., a smooth submanifold in $\mathbb{R}^3$. This is seen by noticing that a point $(z, \bar{z})$ in $M = \mathbb{R}^2$ and the origin is connected by the displacement operator $D(\alpha)$ of coherent states. That is, the existence of differential structure is guaranteed by the unitary operator $U(z, \bar{z})$. This is also consistent with the fact that a coordinate operator $\hat{x}^1$ of the Moyal plane is simultaneously a differential operator $i\theta\partial_2 = [\hat{x}^1, \cdot]$. Thus, it is important to include the information on the connection into the shape $(M, E)$, in order to distinguish these cases.

If several zero modes appear, $M$ consists of several pieces, each of which may have a different dimension in general. In a very particular case, if there are $n$ zero modes that are degenerate on the same region $M$, then $E$ becomes a $U(n)$ bundle over $M$. This is in contrast to the conventional description of D-branes. The difference is apparent when considering fluctuations $\Phi' = \Phi + \delta\Phi$ further. In the conventional description, $\delta\Phi$ is identified as a matrix scalar field on $M$ but, in our treatment, we seek a zero locus again, and obtain another shape $(M', E')$. In this sense, $M$ is always commutative and no matrix scalar fields appear on $M$.

Before going to K-homology, we make a brief comment on the boundary state description of D-branes. A system of coincident D-branes is most rigorously defined by a boundary state equipped with a boundary interaction representing fields on D-branes. In this description, D-branes have a definite position defined by a Dirichlet boundary condition, and matrix scalar fields are treated as boundary perturbations. A bound state of $n$ D2-branes and $k$ D0-branes can be described by either (1) the D2-brane picture: a D2-brane boundary state with a $U(n)$ gauge field $A$ carrying $k$ D0-brane charge, or (2) the D0-brane picture: a D0-brane boundary state with $U(k)$ scalar fields $\Phi$ carrying $n$ D2-brane charge. Schematically, the equivalence of the two pictures is given by

$$e^{-S_b[A]} \,|\, D2 \,\rangle = e^{-S_b[\Phi]} \,|\, D0 \,\rangle. \tag{4.1}$$

In the Moyal case, the equivalence of the two pictures is shown in Refs. [34,35]. Both pictures represent the same mixed boundary condition from different viewpoints: Picture (1) represents it as

a deformation of the Neumann boundary state by a boundary interaction (constant $U(1)$ gauge flux); (2) represents it as that of the Dirichlet boundary state. In terms of tachyon condensation, the system can also be realized by the boundary state of non-BPS D3-branes

$$e^{-S_b[T]} \mid D3 \rangle \tag{4.2}$$

with a tachyon field $T$. The advantage of this realization is that both pictures are two different choices of basis for the tachyon profile and thus they are manifestly unitarily equivalent. The D0-brane picture (2) corresponds to the basis that diagonalizes the ABS construction, and the D2-brane picture (1) corresponds to the basis that diagonalizes the full tachyon profile including $\Phi$.[7] We stress here, however, that the concept of the shape is independent of the choice of pictures (1) and (2). Although the shape in the Moyal case happens to be well described in picture (1), this is just by chance. For generic $\Phi$, although the boundary state (4.2) can be still defined and we can read off the shape and/or the boundary condition from this expression, there is no guarantee that the obtained shape is always well described in a specific picture like (1).

### *4.3. K-homology*

The shape of D0-branes described so far fits nicely with the classification of D-branes by the K-homology group, as noted. In particular, we emphasize that the Myers term can be incorporated in this classification.

Let us recall the definition of the K-homology [38]. A K-cycle for a topological space $X$ is a triple $(M, E, \phi)$, where $M$ is a compact spin$^c$ manifold without boundary, $E \to M$ is a complex vector bundle, and $\phi : M \to X$ is a continuous map. The (topological or geometric) K-homology group is defined by $K_*(X) = \{(M, E, \phi)\}/\sim$, where the equivalence relation is generated by (a) bordism, (b) direct sum, and (c) vector bundle modification defined by the relation that will be shown in Eq. (4.3). Here $* = 0$ (1) corresponds to $M$ with even (odd) dimension, respectively.

Since the K-homology group is a Poincaré dual to the K-theory group, it is natural to conjecture that the K-homology classifies D-branes. This was first described in concrete form in Ref. [39] (see also previous discussions [40,41] and subsequent developments [42–44]). A K-cycle is conjectured to be a D-brane itself, where $M$ is a worldvolume of a BPS Dp-brane[8], $E$ is a Chan–Paton bundle on $M$, and $\phi$ is an embedding of $M$ to the spacetime $X$. The equivalence relations have also been interpreted as physical equivalences: (a) is a continuous deformation of a D-brane, (b) is a gauge symmetry enhancement of coincident D-branes, and (c) is a dielectric effect [39,42,43]. In the following, however, we discuss the idea that we should modify the physical interpretation of the equivalence relation (c).

We start by pointing out that there are several subtleties in the above interpretation. First, since $\phi$ is not necessarily an embedding but just a continuous map, there can be such an $M$ whose dimension is larger than that of $X$ in principle. Therefore, precisely speaking, the physical interpretation described above can be applied only when we implicitly regard $\phi$ as an embedding [45]. Next, there is no room for matrix-valued scalar fields in K-cycles, since only a single scalar field ($U(1)$ part) is implicitly assumed when we consider $\phi$ to be the embedding. As a result, we cannot incorporate the Myers term in this interpretation in particular. The Myers term $\mathrm{Tr} e^{i_\Phi i_\Phi} C$ in the RR-coupling (Chern–Simons term) for D0-branes is originally obtained by applying T-duality to the RR-coupling for D9-branes,

[7] They are analogous to the interaction and the Heisenberg picture, respectively, in quantum mechanics.
[8] More precisely, each connected component of $M$ corresponds to a worldvolume.

which includes the Chern character $C \wedge \mathrm{Tr} e^F$. In the latter case, a non-trivial gauge flux $F \neq 0$ is topologically distinct from $F = 0$, indicating RR-coupling to higher-rank RR-potentials, known as branes within branes [46]. This information is already incorporated as the Chern character for a K-cycle [38] as shown in Ref. [39]. Similarly, since non-commuting scalar fields $\Phi$ produce an RR-coupling to higher-rank RR-potentials through the Myers term, T-duality requires that such a configuration is distinguished from a commuting one. If the K-homology classifies all possible D-branes, it should be able to take into account the matrix scalar fields.

Now, let us turn to the situation in this paper. In the coherent state method, the shape of $k$ D0-branes is a region $M$ in the spatial part $X = \mathbb{R}^3$ of the spacetime, which can naturally be identified with $\phi(M)$ in the K-cycle, with the canonical inclusion map $\phi$. There is also a $U(1)$ Chan–Paton bundle with $k$-magnetic charge. As stated, if the zero loci are degenerate, it is extended to a non-Abelian Chan–Paton bundle $\phi^* E$. Therefore, our shape naturally corresponds to a K-cycle $(M, E, \phi)$, even if the matrix scalar fields $\Phi$ are non-commuting. In particular, the Myers term is implicitly incorporated in this new interpretation.

To see the effect of the Myers term more explicitly, we recall the equivalence (c), the vector bundle modification [38]:

$$(M, E, \phi) \sim (\hat{M}, \hat{H} \otimes \pi^* E, \phi \circ \pi). \tag{4.3}$$

The r.h.s. is obtained from the l.h.s. through the clutching construction: $\pi : \hat{M} \to M$ is a sphere bundle over $M$ whose fiber is an even-dimensional sphere $S^{2n}$. $\hat{H} \to \hat{M}$ is a complex vector bundle over $\hat{M}$ whose fiber is a Bott generator on $S^{2n}$. Because of the appearance of the sphere, $\hat{M}$ has been interpreted as the worldvolume of a spherical D-brane [39,42,43]. However, as seen by following Ref. [38] carefully, we should rather interpret $\hat{M}$ as a worldvolume of the D$\bar{\text{D}}$-system and $\hat{H}$ as an ABS construction representing $M$ as a codimension-$2n$ soliton in $\mathbb{R}^{2n}$ (whose one-point compactification is $S^{2n}$ above). In other words, the equivalence (4.3) should be just a physical equivalence between a D-brane and the same D-brane constructed by the tachyon condensation. This is consistent with the fact that the image of both maps $\phi(M) = \phi \circ \pi(\hat{M})$ represents the same region in $X$ and the fiber $S^{2n}$ is not seen in $X$.

In our situation, the K-cycle $(M_0, E_0, \phi_0)$ on the l.h.s. of Eq. (4.3) corresponds to $k$ D0-branes without scalar fields; $\Phi = 0$. That is, $M_0$ is a point, $\phi_0(M_0) = 0$ in $X = \mathbb{R}^3$ and $E_0 = \mathbb{C}^k$ is a Chan–Paton space. It is equivalent to the r.h.s. of Eq. (4.3), where $\hat{M}_0 = S^4$ (the one-point compactification of $\mathbb{R}^4$) and $\hat{H}_0$ is an ABS construction of the codimension-4 soliton on the D4$\bar{\text{D}}$4-system. Note that our non-BPS D3-branes are considered as part of this system given by a kink solution along the $x^4$-direction. Thus, $\hat{H}_0$ here is essentially given by Eq. (2.1) with $\Phi = 0$.

Let us turn to the case of adding matrix scalar fields $\Phi$. Under the present interpretation, the deformation of $(M_0, E_0, \phi_0)$ by $\Phi$ (with a non-zero Myers term) is naturally realized as the deformation of the r.h.s. with the tachyon profile (2.1) with $\Phi$. The obtained K-cycle can be non-equivalent to the point-like K-cycle from the above argument. In that case, it should rather be equivalent to another K-cycle that is given by the shape of D0-branes with $\Phi$. In our examples, we obtain a triple $(M_1, E_1, \phi_1)$, where $M_1 = S^2$ (in the Moyal case, one-point compactification of $\mathbb{R}^2$), $E_1$ is a $U(1)$ Chan–Paton bundle with magnetic flux $k$, and $\phi_1 : S^2 \to X$. Although the non-equivalence between $(M_0, E_0, \phi_0)$ and $(M_1, E_1, \phi_1)$ should be proven mathematically, it should be consistent with the structure of solitons and the RR-coupling described above.

In summary, we propose that the shape of D0-branes with scalar fields corresponds to a K-cycle. We claim that the Myers term (non-commuting scalar fields) is incorporated as a non-equivalent deformation of K-cycles rather than the vector bundle modification.

## 5. Conclusion and discussion

We considered D-brane systems with non-commuting scalar fields $\Phi$ via tachyon condensation and gave a novel prescription to read off the shape of the non-commutative D-brane system as a commutative region in spacetime, by rearranging the idea of the method proposed in Refs. [12,17,19] (the coherent state method) as tachyon condensation. In this interpretation, the shape of the D-brane is defined as a set of zeros of the tachyon field together with a gauge flux on it. We also argued that the shapes fit well with the classification of D-branes by the K-homology group. This shows that the D-branes made through the Myers term are incorporated in this classification.

As typical examples, we closely investigated the Moyal plane and the fuzzy sphere but generalization to other systems is straightforward. The point is that we can always diagonalize a tachyon profile for any matrix-valued scalar fields $\Phi$ that do not need to satisfy the equation of motion of the effective theory on D0-branes and/or the superstring theory. Although we focus in this paper on the universality of our method, by which we can define the shape for arbitrary configuration of $\Phi$, it would be an interesting problem to characterize the shapes that are also classical solutions of superstring theory.

Since we focused mainly on the topological aspects of the shape $M$ corresponding to the K-homology, there are several issues that we did not touch upon. In this section, we briefly discuss two other aspects of the shape.

### *5.1. Metric on the shape*

From the point of view of the coherent state method, it is natural to define a metric of the shape only from the matrices $\Phi$ [17,18]. In the present context, it is suitable to be defined on the zero mode of the Chan–Paton bundle. There are several notions of metrics defined on a family of Hilbert spaces, such as the quantum Fisher metric, the Fubini–Study metric, and the fidelity susceptibility. Here we adopt the definition of Refs. [47,48].

Let $|\,\psi(q)\,\rangle$ be a state depending on external parameters denoted by $q^i$. In the information theoretic geometry, the metric on the parameter space is defined by

$$g_{ij} = \mathrm{Re}(C_{ij} - A_i A_j), \tag{5.1}$$

where the quantities $C_{ij}$ and $A_i$ are

$$\begin{aligned} &C_{ij}(q)dq^i dq^j = |\psi(q+dq) - \psi(q)|^2 = \left\langle\, \partial_i\psi(q) \,|\, \partial_j\psi(q) \,\right\rangle dq^i dq^j, \\ &A_i(q) = -i\,\langle\, \psi(q) \,|\, \partial_i\psi(q)\,\rangle. \end{aligned} \tag{5.2}$$

In our case, a tachyon zero mode has the form $|\,\psi_0(\boldsymbol{x})\,\rangle = U(\boldsymbol{x})\,|\,0\,\rangle$, where $\boldsymbol{x} \in \mathbb{R}^3$ are considered to be parameters and $U(\boldsymbol{x})$ is determined by $\Phi$. Then, the above quantities are written as

$$C_{ij}(\boldsymbol{x}) = \langle\, 0 \,|\, \partial_i U(\boldsymbol{x})^\dagger \partial_j U(\boldsymbol{x}) \,|\, 0\,\rangle, \quad A_i(\boldsymbol{x}) = -i\,\langle\, 0 \,|\, U(\boldsymbol{x})^\dagger \partial_i U(\boldsymbol{x}) \,|\, 0\,\rangle. \tag{5.3}$$

The latter is nothing but the induced gauge potential (2.12). This metric gives a length between zero mode states $|\,\psi_0(\boldsymbol{x})\,\rangle$ and $|\,\psi_0(\boldsymbol{x}+d\boldsymbol{x})\,\rangle$ at two nearby points[9] essentially through the overlap

[9] Of course, they should belong to the same open set in $M$.

$\langle\, \psi_0(\boldsymbol{x}+d\boldsymbol{x}) \,|\, \psi_0(\boldsymbol{x}) \,\rangle$. In other words, this length is defined along the fiber direction of the Chan–Paton bundle.

Applying this to the Moyal case, we obtain (see Appendix A.1 for a proof)

$$C_{ij}(z,\bar{z}) = \langle\, 0,+ \,|\, \partial_i U(z)^\dagger \partial_j U(z) \,|\, 0,+ \,\rangle = \langle\, 0 \,|\, \partial_i D(\alpha)^\dagger \partial_j D(\alpha) \,|\, 0 \,\rangle, \tag{5.4}$$

$$A_i(z,\bar{z}) = -i \langle\, 0,+ \,|\, U(z)^\dagger \partial_i U(z) \,|\, 0,+ \,\rangle = -i \langle\, 0 \,|\, D(\alpha)^\dagger \partial_i D(\alpha) \,|\, 0 \,\rangle, \tag{5.5}$$

and the metric becomes

$$ds^2 = d\alpha d\bar{\alpha} = \frac{1}{2\theta} dz d\bar{z}. \tag{5.6}$$

This is a flat metric on $\mathbb{R}^2$ but different from the induced metric of the flat Euclidean background by a Weyl factor.

For the fuzzy sphere case, the quantities in Eq. (5.3) should be evaluated patch-wise with respect to the state $R_N(\Omega) \,|\, \ell,+ \,\rangle$ on $\mathcal{U}_N$ and $R_S(\Omega) \,|\, \ell,+ \,\rangle$ on $\mathcal{U}_S$, respectively. It turns out, however, that the line element is the same in both $\mathcal{U}_N$ and $\mathcal{U}_S$ (see Appendix A.4):

$$ds^2 = \frac{1}{2}\left(\ell + \frac{1}{2}\right)\left(d\theta^2 + \sin^2\theta d\varphi^2\right) = \frac{k}{4} d^2\Omega. \tag{5.7}$$

This is the round metric on $S^2$ with a Weyl factor. This metric should be compared with two alternative metrics: the induced metric of the sphere with radius $|\boldsymbol{x}| = \rho\ell$, $ds^2 = \rho^2\ell^2 d^2\Omega$, and the metric of the fuzzy sphere with radius $\rho\sqrt{\ell(\ell+1)}$, $ds^2 = \rho^2\ell(\ell+1)d^2\Omega$. Again, the information metric (5.7) is different from both of them by a Weyl factor.

Although the difference between the information metric and the induced metric of the flat target space is only the Weyl factors in these examples, this is not the case in general. This can be most easily checked by adding perturbations to $\Phi$ in both examples. This difference can also be intuitively understood as follows. In the above examples, the Weyl factors are given by the inverse of the non-commutative parameters, which are also related to the densities of the D0-branes. The induced metric just depends on the shape in the target space, while the information metric picks up information on the density distribution of D0-branes. At least in the large-$N$ limit, there exist two configurations of D0-branes such that they have a common shape in the target space but have different density distributions. Such two configurations will share the same induced metric but have different information metrics. This implies the inequivalence of the two metrics.

The appearance of the non-commutative parameters in the information metric also suggests that the information metric is the Kähler metric associated with the symplectic structure given by the gauge flux. In the above examples, the information metrics are indeed the Kähler metrics. In Ref. [18], it is also shown for a wide class of matrix configurations that the information metric is indeed reduced to the Kähler metric in the large-$N$ limit.

### 5.2. *Effective theory on the shape*

We close this paper with a rather speculative discussion. We come back to the example of the fuzzy sphere. The shape $(M, E)$ in this case is given by $M = S^2$ and $E$ is a complex line bundle over $M$ equipped with the $k$-monopole connection. This connection comes from displacements of the Bloch coherent states and this suggests that a smooth structure is guaranteed to exist. However, the situation is different from the Moyal case, because the fuzzy sphere is made of finite matrices. This is easily seen by considering algebra of functions on a fuzzy sphere and a commutative sphere.

The algebra of functions on a fuzzy sphere is called fuzzy spherical harmonics, which corresponds to ordinary spherical harmonics with a restriction in the maximal angular momentum in order to match the degrees of freedom[10]. In order to close the latter algebra by restricted harmonics, it is necessary to deform the product to a non-commutative one ($*$-product). Although our shape $S^2$ is a commutative region in spacetime, when considering functions on it, this suggests that it behaves as a non-commutative space.

This is not a contradiction because the function algebra is needed only if we consider an effective field theory on the shape. Of course, we do not need to consider a fluctuation as transverse scalar fields on the shape as stated before. When the fuzzy sphere configuration $\Phi$ corresponds to the shape $(M = S^2, E)$, then adding fluctuations $\Phi' = \Phi + \delta\Phi$ gives another shape $(M', E')$. However, it would also be convenient to find the effective theory description, as in the conventional D2-brane picture. That is, the shape is kept as $(M, E)$ but $\delta\Phi$ is treated as a field on the shape.

To find a new shape caused by a small fluctuation, the standard perturbation theory in quantum mechanics can be applied. The perturbed tachyon profile $T[\Phi']$ can be considered as a Dirac-like operator with an interaction term $u\boldsymbol{\sigma} \cdot \delta\Phi$. Then, the new zero mode of $T[\Phi']$ will be given by a linear combination of the ONB for unperturbed $T[\Phi]$. For this purpose, the complete set of ONB found in this paper can be used.

In the language of the boundary state, this procedure is understood as follows. The boundary state of the D0-brane picture is $e^{-S_b[\Phi']}\,|\,D0\,\rangle$ with scalar fields $\Phi' = \Phi + \delta\Phi$. By realizing it as the D3-brane boundary state (4.2), it would be rewritten as the form $e^{-S_b[\delta\Phi]}\,|\,M, E\,\rangle$. Here the state $|\,M, E\,\rangle$ corresponds to the shape $M = S^2$ for a fuzzy sphere. It would not be the conventional Neumann boundary state along the $S^2$ direction, but will be a variant of the mixed boundary state, if the shape behaves as a non-commutative space. The field on the shape $S^2$ is extracted by the boundary interaction $e^{-S_b[\delta\Phi]}$. It is interesting to see whether the effective theory for $\delta\Phi$ is given by a non-commutative field theory on $M = S^2$ with a $*$-product. This problem is closely related to the situation of the Seiberg–Witten map [49]. It will be interesting to study fluctuations around the Moyal plane and the fuzzy sphere and investigate the relation to the Seiberg–Witten map. We hope to report on this issue in the near future.

**Acknowledgements**

We would like to thank S. Terashima for useful discussions and comments. The work of G.I. was supported in part by the Program to Disseminate Tenure Tracking System, MEXT, Japan and by KAKENHI (16K17679). The work of S.M. was supported in part by a Grant-in-Aid for Scientific Research (C) 15K05060.

**Funding**

Open Access funding: SCOAP[3].

## A. Computational details

### *A.1. Gauge flux and metric for the Moyal case*

For the displacement operator (3.7), we first show the relations

$$\partial_\alpha D(\alpha) = D(\alpha)(\hat{a}^\dagger + \tfrac{\bar{\alpha}}{2}), \qquad \partial_{\bar{\alpha}} D(\alpha) = -D(\alpha)(\hat{a} + \tfrac{\alpha}{2}), \tag{A.1}$$

$$\partial_\alpha D^\dagger(\alpha) = -(\hat{a}^\dagger + \tfrac{\bar{\alpha}}{2})D^\dagger(\alpha), \qquad \partial_{\bar{\alpha}} D^\dagger(\alpha) = (\hat{a} + \tfrac{\alpha}{2})D^\dagger(\alpha), \tag{A.2}$$

[10] In our case, because a monopole exists, it is better to think about (fuzzy) monopole harmonics.

and then calculate a gauge potential and a metric. To this end, we will use an identity

$$\frac{d}{dt}e^{B(t)} = e^{B(t)}d\exp_{-B(t)}(B'(t)), \tag{A.3}$$

which is valid for any operator $B(t)$ with a parameter $t$. Here $B'(t) = \frac{d}{dt}B(t)$ and

$$d\exp_B(C) = \sum_{l=0}^{\infty}\frac{1}{(l+1)!}(\mathrm{ad}_B)^l(C) = \frac{e^{\mathrm{ad}_B}-\mathrm{id.}}{\mathrm{ad}_B}(C). \tag{A.4}$$

First we set $B(\alpha) = \alpha\hat{a}^\dagger - \bar{\alpha}\hat{a}$. Then, we have $\partial_\alpha B(\alpha) = \hat{a}^\dagger$ and

$$\mathrm{ad}_{-B}(\partial_\alpha B) = [-\alpha\hat{a}^\dagger + \bar{\alpha}\hat{a}, \hat{a}^\dagger] = \bar{\alpha}. \tag{A.5}$$

The higher-order terms $(\mathrm{ad}_{-B})^l(\partial_\alpha B)$ $(l \geq 2)$ vanish so that Eq. (A.4) becomes

$$d\exp_{-B}(\partial_\alpha B) = \hat{a}^\dagger + \tfrac{1}{2}\bar{\alpha}, \tag{A.6}$$

and we obtain

$$\partial_\alpha D(\alpha) = D(\alpha)(\hat{a}^\dagger + \tfrac{1}{2}\bar{\alpha}). \tag{A.7}$$

Similarly, by setting $B(\bar{\alpha}) = \alpha\hat{a}^\dagger - \bar{\alpha}\hat{a}$, we have $\partial_{\bar{\alpha}}B = -\hat{a}$ and

$$\begin{aligned} &\mathrm{ad}_{-B}(\partial_{\bar{\alpha}}B) = [-\alpha\hat{a}^\dagger + \bar{\alpha}\hat{a}, -\hat{a}] = -\alpha, \\ \Rightarrow\ &d\exp_{-B}(\partial_{\bar{\alpha}}B) = -\hat{a} - \tfrac{1}{2}\alpha, \\ \Rightarrow\ &\partial_{\bar{\alpha}}D(\alpha) = -D(\alpha)(\hat{a} + \tfrac{1}{2}\alpha). \end{aligned} \tag{A.8}$$

The others in Eq. (A.2) are obtained by $\partial D^\dagger = -D^\dagger\partial DD^\dagger$. For the gauge potential, because of $\alpha = z/\sqrt{2\theta}$, we need to estimate

$$\begin{aligned} dD(\alpha) &= dz\partial_z D(\alpha) + d\bar{z}\partial_{\bar{z}}D(\alpha) \\ &= d\alpha\partial_\alpha D(\alpha) + d\bar{\alpha}\partial_{\bar{\alpha}}D(\alpha). \end{aligned} \tag{A.9}$$

By using Eq. (A.1), we obtain

$$\begin{aligned} A_\alpha &= -i\,\langle\,0\,|\,D^\dagger(\alpha)\partial_\alpha D(\alpha)\,|\,0\,\rangle = -i\,\langle\,0\,|\,\hat{a}^\dagger + \tfrac{\bar{\alpha}}{2}\,|\,0\,\rangle = -i\tfrac{\bar{\alpha}}{2}, \\ A_{\bar{\alpha}} &= -i\,\langle\,0\,|\,D^\dagger(\alpha)\partial_{\bar{\alpha}}D(\alpha)\,|\,0\,\rangle = i\,\langle\,0\,|\,\hat{a} + \tfrac{\alpha}{2}\,|\,0\,\rangle = i\tfrac{\alpha}{2}, \end{aligned} \tag{A.10}$$

and thus

$$A = A_\alpha d\alpha + A_{\bar{\alpha}}d\bar{\alpha} = -\frac{i}{2}(\bar{\alpha}d\alpha - \alpha d\bar{\alpha}) = -\frac{i}{4\theta}(\bar{z}dz - zd\bar{z}). \tag{A.11}$$

Next we calculate the metric. In Eq. (5.3), $A_i$ is given by Eq. (A.10) and $C_{ij}$ is obtained as

$$\begin{aligned} C_{\alpha\alpha} &= \langle\,0\,|\,\partial_\alpha D^\dagger(\alpha)\partial_\alpha D(\alpha)\,|\,0\,\rangle = -\,\langle\,0\,|\,(\hat{a}^\dagger + \tfrac{\bar{\alpha}}{2})^2\,|\,0\,\rangle = -\tfrac{\bar{\alpha}^2}{4}, \\ C_{\bar{\alpha}\bar{\alpha}} &= \langle\,0\,|\,\partial_{\bar{\alpha}} D^\dagger(\alpha)\partial_{\bar{\alpha}} D(\alpha)\,|\,0\,\rangle = -\,\langle\,0\,|\,(\hat{a} + \tfrac{\alpha}{2})^2\,|\,0\,\rangle = -\tfrac{\alpha^2}{4}, \\ C_{\alpha\bar{\alpha}} &= \langle\,0\,|\,\partial_\alpha D^\dagger(\alpha)\partial_{\bar{\alpha}} D(\alpha)\,|\,0\,\rangle = \langle\,0\,|\,(\hat{a} + \tfrac{\alpha}{2})(\hat{a}^\dagger + \tfrac{\bar{\alpha}}{2})\,|\,0\,\rangle = \tfrac{|\alpha|^2}{4} + 1, \\ C_{\bar{\alpha}\alpha} &= \langle\,0\,|\,\partial_{\bar{\alpha}} D^\dagger(\alpha)\partial_\alpha D(\alpha)\,|\,0\,\rangle = \langle\,0\,|\,(\hat{a}^\dagger + \tfrac{\bar{\alpha}}{2})(\hat{a} + \tfrac{\alpha}{2})\,|\,0\,\rangle = \tfrac{|\alpha|^2}{4}. \end{aligned} \tag{A.12}$$

By using these, the components in the metric are

$$\begin{aligned} g_{\alpha\alpha} &= -\frac{\bar{\alpha}^2}{4} + \frac{\bar{\alpha}^2}{4} = 0, \\ g_{\bar{\alpha}\bar{\alpha}} &= -\frac{\alpha^2}{4} + \frac{\alpha^2}{4} = 0, \\ g_{\alpha\bar{\alpha}} &= \frac{|\alpha|^2}{4} + 1 - \frac{|\alpha|^2}{4} = 1, \\ g_{\bar{\alpha}\alpha} &= \frac{|\alpha|^2}{4} - \frac{|\alpha|^2}{4} = 0, \end{aligned} \tag{A.13}$$

and thus the line element becomes

$$ds^2 = d\alpha d\bar{\alpha}. \tag{A.14}$$

### *A.2. Rotation*

Let $\Lambda$ be the rotation matrix that sends $\boldsymbol{x} = (x^1, x^2, x^3)$ to $\boldsymbol{x} = (0, 0, r)$, and let $R$ be the corresponding unitary operator such that

$$\Lambda^i_j J^j = R^\dagger J_i R. \tag{A.15}$$

We have two possibilities:

(a) Rotation about an axis $\boldsymbol{n} = (-\sin\varphi, \cos\varphi, 0)$ with an angle $-\theta$.
(b) The sequence of (1) rotation about an axis $\boldsymbol{n} = (0, 0, 1)$ with an angle $-\varphi$, (2) rotation about an axis $\boldsymbol{n} = (0, 1, 0)$ with an angle $-\theta$, and (3) rotation about an axis $\boldsymbol{n} = (0, 0, 1)$ with an angle $\varphi$.

We will see (b) first. Operation (1) is generated by $R_1 = e^{i(-\varphi)J_3} = e^{-i\varphi J_3}$. In fact,

$$\begin{aligned} R_1^\dagger J_1 R_1 &= e^{i\varphi J_3} J_1 e^{-i\varphi J_3} = \cos\varphi J_1 - \sin\varphi J_2, \\ R_1^\dagger J_2 R_1 &= e^{i\varphi J_3} J_2 e^{-i\varphi J_3} = \cos\varphi J_2 + \sin\varphi J_1, \\ R_1^\dagger J_3 R_1 &= e^{i\varphi J_3} J_3 e^{-i\varphi J_3} = J_3, \end{aligned} \tag{A.16}$$

which means

$$\Lambda_1 = \begin{pmatrix} \cos\varphi & -\sin\varphi & 0 \\ \sin\varphi & \cos\varphi & 0 \\ 0 & 0 & 1 \end{pmatrix}. \tag{A.17}$$

Operation (2) is generated by $R_2 = e^{i(-\theta)J_2} = e^{-i\theta J_2}$. In fact,

$$\begin{aligned} R_2^\dagger J_1 R_2 &= e^{i\theta J_2} J_1 e^{-i\theta J_2} = \cos\theta J_1 + \sin\theta J_3, \\ R_2^\dagger J_2 R_2 &= e^{i\theta J_2} J_2 e^{-i\theta J_2} = J_2, \\ R_2^\dagger J_3 R_2 &= e^{i\theta J_2} J_3 e^{-i\theta J_2} = \cos\theta J_3 - \sin\theta J_1, \end{aligned} \tag{A.18}$$

which means

$$\Lambda_2 = \begin{pmatrix} \cos\theta & 0 & \sin\theta \\ 0 & 1 & 0 \\ -\sin\theta & 0 & \cos\theta \end{pmatrix}. \tag{A.19}$$

Operation (3) is generated by $R_3 = e^{i\varphi J_3}$. In fact,

$$\begin{aligned} R_3^\dagger J_1 R_3 &= e^{-i\varphi J_3} J_1 e^{i\varphi J_3} = \cos\varphi J_1 + \sin\varphi J_2, \\ R_3^\dagger J_2 R_3 &= e^{-i\varphi J_3} J_2 e^{i\varphi J_3} = \cos\varphi J_2 - \sin\varphi J_1, \\ R_3^\dagger J_3 R_3 &= e^{-i\varphi J_3} J_3 e^{i\varphi J_3} = J_3, \end{aligned} \tag{A.20}$$

which means

$$\Lambda_3 = \begin{pmatrix} \cos\varphi & \sin\varphi & 0 \\ -\sin\varphi & \cos\varphi & 0 \\ 0 & 0 & 1 \end{pmatrix}. \tag{A.21}$$

Then the sequence of (1) to (3) is generated by $R = R_1 R_2 R_3$ and

$$\Lambda = \Lambda_1\Lambda_2\Lambda_3 = \begin{pmatrix} \cos\varphi & -\sin\varphi & 0 \\ \sin\varphi & \cos\varphi & 0 \\ 0 & 0 & 1 \end{pmatrix} \begin{pmatrix} \cos\theta & 0 & \sin\theta \\ 0 & 1 & 0 \\ -\sin\theta & 0 & \cos\theta \end{pmatrix} \begin{pmatrix} \cos\varphi & \sin\varphi & 0 \\ -\sin\varphi & \cos\varphi & 0 \\ 0 & 0 & 1 \end{pmatrix}. \tag{A.22}$$

On the other hand, $R$ is rewritten as

$$\begin{aligned} R &= R_1 R_2 R_3 = e^{-i\varphi J_3} e^{-i\theta J_2} e^{i\varphi J_3} \\ &= \exp(-i\theta e^{-i\varphi J_3} J_2 e^{i\varphi J_3}) = e^{-i\theta(\cos\varphi J_2 - \sin\varphi J_1)} = e^{i(-\theta)(-\sin\varphi J_1 + \cos\varphi J_2)}, \end{aligned} \tag{A.23}$$

which says that $R$ generates (a). By using $J_\pm = J_1 \pm iJ_2$, $R$ is also written as

$$R = e^{-\frac{1}{2}\theta(e^{-i\varphi}J_+ - e^{i\varphi}J_-)}. \tag{A.24}$$

### *A.2.1. The case of spin* $\frac{1}{2}$

The unitary operator $R$ in this case is given by

$$\begin{aligned} R &= e^{-i\varphi S_3} e^{-i\theta S_2} e^{i\varphi S_3} = e^{-i\frac{\varphi}{2}\sigma_3} e^{-i\frac{\theta}{2}\sigma_2} e^{i\frac{\varphi}{2}\sigma_3} \\ &= \begin{pmatrix} e^{-i\frac{\varphi}{2}} & 0 \\ 0 & e^{i\frac{\varphi}{2}} \end{pmatrix} \begin{pmatrix} \cos\frac{\theta}{2} & -\sin\frac{\theta}{2} \\ \sin\frac{\theta}{2} & \cos\frac{\theta}{2} \end{pmatrix} \begin{pmatrix} e^{i\frac{\varphi}{2}} & 0 \\ 0 & e^{-i\frac{\varphi}{2}} \end{pmatrix} \\ &= \begin{pmatrix} \cos\frac{\theta}{2} & -\sin\frac{\theta}{2}e^{-i\varphi} \\ \sin\frac{\theta}{2}e^{i\varphi} & \cos\frac{\theta}{2} \end{pmatrix}. \end{aligned} \tag{A.25}$$

## *A.3. Details of the diagonalization*

In general, a $2 \times 2$ matrix of the form $M = M_0\mathbf{1}_2 + M_i\sigma^i$ has eigenvalues $\lambda_\pm = M_0 \pm |M|$, and is diagonalized either by

$$W_1 = \frac{1}{\sqrt{2|M|(|M| + M_3)}} \begin{pmatrix} |M| + M_3 & -M_1 + iM_2 \\ M_1 + iM_2 & |M| + M_3 \end{pmatrix}, \tag{A.26}$$

if $|M| + M_3 \neq 0$, or

$$W_2 = \frac{1}{\sqrt{2|M|(|M| - M_3)}} \begin{pmatrix} M_1 - iM_2 & |M| - M_3 \\ |M| - M_3 & -M_1 - iM_2 \end{pmatrix}, \tag{A.27}$$

if $|M| - M_3 \neq 0$, where $|M| = \sqrt{M_i M^i}$. That is, $M$ is written as

$$M = W_{1,2} \begin{pmatrix} \lambda_+ & 0 \\ 0 & \lambda_- \end{pmatrix} W_{1,2}^\dagger. \tag{A.28}$$

The eigenstates $v_\pm$ with eigenvalues $\lambda_\pm$ are given by two column vectors in $W_1$ (and similar for $W_2$):

$$v_+ = \frac{1}{\sqrt{2|M|(|M|+M_3)}} \begin{pmatrix} |M|+M_3 \\ M_1 + iM_2 \end{pmatrix}, \quad v_- = \frac{1}{\sqrt{2|M|(|M|+M_3)}} \begin{pmatrix} -M_1 + iM_2 \\ |M|+M_3 \end{pmatrix}. \tag{A.29}$$

In our case, $T^{(m)}$ in Eq. (3.44) is written in this form by

$$\begin{aligned} &T^{(m)} = u(M_0^{(m)} \mathbf{1}_2 + M_i^{(m)} \sigma^i), \\ &M_0^{(m)} = \tfrac{\rho}{2}, \quad M_1^{(m)} = -\rho\sqrt{(\ell-m)(\ell+m+1)}, \quad M_2^{(m)} = 0, \quad M_3^{(m)} = |\boldsymbol{x}| - \rho(m+\tfrac{1}{2}). \end{aligned} \tag{A.30}$$

Then, the eigenvalues $\lambda_\pm^{(m)}$ of $T^{(m)}$ are

$$\begin{aligned} \lambda_\pm^{(m)}(|\boldsymbol{x}|) &= u(M_0^{(m)} \pm |M^{(m)}|) \\ &= u\left[\tfrac{\rho}{2} \pm \sqrt{\rho^2(\ell-m)(\ell+m+1) + \left(|\boldsymbol{x}| - \rho(m+\tfrac{1}{2})\right)^2}\right], \end{aligned} \tag{A.31}$$

where we have used

$$|M^{(m)}|^2 = M_i^{(m)} M^{(m)i} = \rho^2(\ell-m)(\ell+m+1) + \left(|\boldsymbol{x}| - \rho(m+\tfrac{1}{2})\right)^2. \tag{A.32}$$

Note that it is also written as

$$M_i^{(m)} M^{(m)i} = |\boldsymbol{x}|^2 - 2\rho|\boldsymbol{x}|\left(m+\tfrac{1}{2}\right) + \rho^2\left(\ell+\tfrac{1}{2}\right)^2. \tag{A.33}$$

Next, we will check whether $W_{1,2}$ in Eqs. (A.26) and (A.27) are allowed. Because $|M^{(m)}|^2 = (M_1^{(m)})^2 + (M_3^{(m)})^2$, we have

$$\begin{aligned} |M^{(m)}| = M_3^{(m)} &\Leftrightarrow |M^{(m)}|^2 = (M_3^{(m)})^2 \text{ and } M_3^{(m)} > 0 \\ &\Leftrightarrow (M_1^{(m)})^2 = 0 \text{ and } M_3^{(m)} > 0, \\ |M^{(m)}| = -M_3^{(m)} &\Leftrightarrow |M^{(m)}|^2 = (M_3^{(m)})^2 \text{ and } M_3^{(m)} < 0 \\ &\Leftrightarrow (M_1^{(m)})^2 = 0 \text{ and } M_3^{(m)} < 0. \end{aligned} \tag{A.34}$$

Since $(M_1^{(m)})^2 \neq 0$ in our case, both $W_1$ and $W_2$ are allowed. Note that, in our definition (A.30), $u$ is extracted, but Eqs. (A.26) and (A.27) are still correct and are $u$-independent. We choose $W_1$, i.e.,

$$\begin{aligned} &T^{(m)} = W^{(m)} \begin{pmatrix} \lambda_+^{(m)} & 0 \\ 0 & \lambda_-^{(m)} \end{pmatrix} W^{(m)\dagger}, \\ &W^{(m)} = \begin{pmatrix} W_{11}^{(m)} & W_{12}^{(m)} \\ W_{21}^{(m)} & W_{22}^{(m)} \end{pmatrix} = \frac{1}{\sqrt{C^{(m)}}} \begin{pmatrix} |M^{(m)}| + M_3^{(m)} & -M_1^{(m)} \\ M_1^{(m)} & |M^{(m)}| + M_3^{(m)} \end{pmatrix}, \end{aligned} \tag{A.35}$$

where we define $C^{(m)} = 2|M^{(m)}|(|M^{(m)}| + M_3^{(m)})$. As an operator, $W^{(m)}$ is written as

$$\begin{aligned} W^{(m)} =& W_{11}^{(m)} \,|\, m,+\rangle\langle m,+\,| + W_{12}^{(m)} \,|\, m+1,-\rangle\langle m,+\,| \\ &+ W_{21}^{(m)} \,|\, m,+\rangle\langle m+1,-\,| + W_{22}^{(m)} \,|\, m+1,-\rangle\langle m+1,-\,|. \end{aligned} \tag{A.36}$$

Then two eigenvalues of $T$ and the corresponding eigenstates are given by

$$\begin{aligned} \lambda_+^{(m)} :&\ \ R_N(\Omega)\left\{W_{11}^{(m)} \,|\, m,+\rangle + W_{21}^{(m)} \,|\, m+1,-\rangle\right\}, \\ \lambda_-^{(m)} :&\ \ R_N(\Omega)\left\{W_{12}^{(m)} \,|\, m,+\rangle + W_{22}^{(m)} \,|\, m+1,-\rangle\right\}. \end{aligned} \tag{A.37}$$

For later purposes, we define a unitary operator $W_N$, which acts as $W^{(m)}$ on each subspace $\mathrm{span}\{|\, m,+\rangle, |\, m+1,-\rangle\}$ for $m$, and 1 for $|\, \ell,+\rangle$ and $|\, -\ell,-\rangle$:

$$W_N(|\boldsymbol{x}|) = |\, \ell,+\rangle\langle \ell,+\,| + |\, -\ell,-\rangle\langle -\ell,-\,| + \sum_{m=-\ell}^{\ell-1} W^{(m)}. \tag{A.38}$$

This depends on $|\boldsymbol{x}|$ but is independent of $\Omega$. Then, the tachyon field is written as

$$T(\boldsymbol{x}) = W_N(|\boldsymbol{x}|)R_N(\Omega)\Lambda(|\boldsymbol{x}|)R_N^\dagger(\Omega)W_N^\dagger(|\boldsymbol{x}|), \tag{A.39}$$

where $\Lambda$ denotes a Hermitian operator of eigenvalues:

$$\begin{aligned} \Lambda(|\boldsymbol{x}|) =& u(|\boldsymbol{x}| - \rho\ell)\,|\, \ell,+\rangle\langle \ell,+\,| - u(|\boldsymbol{x}| + \rho\ell)\,|\, -\ell,-\rangle\langle -\ell,-\,| \\ &+ \sum_{m=-\ell}^{\ell-1} \lambda_+^{(m)} \,|\, m,+\rangle\langle m,+\,| + \lambda_-^{(m)} \,|\, m+1,-\rangle\langle m+1,-\,|. \end{aligned} \tag{A.40}$$

### *A.4. Gauge flux and metric for the fuzzy sphere case*

#### *A.4.1. In the open set $\mathcal{U}_N$*

For Eq. (3.34), we first show the relations

$$\partial_\theta R_N(\Omega) = R_N(\Omega)\tfrac{1}{2}(e^{i\varphi}J_- - e^{-i\varphi}J_+), \tag{A.41}$$

$$\partial_\theta R_N^\dagger(\Omega) = -\tfrac{1}{2}(e^{i\varphi}J_- - e^{-i\varphi}J_+)R_N^\dagger(\Omega), \tag{A.42}$$

$$\partial_\varphi R_N(\Omega) = R_N(\Omega)\left[i(1-\cos\theta)J_3 + \tfrac{i}{2}\sin\theta(e^{i\varphi}J_- + e^{-i\varphi}J_+)\right], \tag{A.43}$$

$$\partial_\varphi R_N^\dagger(\Omega) = -\left[i(1-\cos\theta)J_3 + \tfrac{i}{2}\sin\theta(e^{i\varphi}J_- + e^{-i\varphi}J_+)\right]R_N^\dagger(\Omega). \tag{A.44}$$

Equations (A.42) and (A.44) follow from Eqs. (A.41) and (A.43), respectively. To show Eqs. (A.41) and (A.43), we will use the identity (A.3) again. By setting $B(\theta,\varphi) = \frac{1}{2}\theta(e^{i\varphi}J_- - e^{-i\varphi}J_+)$, we have

$$\begin{aligned} \partial_\theta B(\theta,\varphi) &= \tfrac{1}{2}(e^{i\varphi}J_- - e^{-i\varphi}J_+), \\ \partial_\varphi B(\theta,\varphi) &= \tfrac{i}{2}\theta(e^{i\varphi}J_- + e^{-i\varphi}J_+). \end{aligned} \tag{A.45}$$

From the first line of Eq. (A.45), it is obvious that

$$\mathrm{ad}_{-B}(\partial_\theta B) = [-\tfrac{1}{2}\theta(e^{i\varphi}J_- - e^{-i\varphi}J_+), \tfrac{1}{2}(e^{i\varphi}J_- - e^{-i\varphi}J_+)] = 0, \tag{A.46}$$

and that the higher-order terms vanish. Thus, we find

$$R_N^\dagger(\Omega)\partial_\theta R_N(\Omega) = d\exp_{-B}(\partial_\theta B) = \tfrac{1}{2}(e^{i\varphi}J_- - e^{-i\varphi}J_+), \tag{A.47}$$

which leads to Eq. (A.41). From the second line of Eq. (A.45), we find

$$\begin{aligned}\mathrm{ad}_{-B}(\partial_\varphi B) &= [-\tfrac{1}{2}\theta(e^{i\varphi}J_- - e^{-i\varphi}J_+), \tfrac{i}{2}\theta(e^{i\varphi}J_- + e^{-i\varphi}J_+)] \\ &= -\tfrac{i}{4}\theta^2[e^{i\varphi}J_- - e^{-i\varphi}J_+, e^{i\varphi}J_- + e^{-i\varphi}J_+] \\ &= i\theta^2 J_3,\end{aligned} \tag{A.48}$$

and

$$\begin{aligned}(\mathrm{ad}_{-B})^2(\partial_\varphi B) &= [-\tfrac{1}{2}\theta(e^{i\varphi}J_- - e^{-i\varphi}J_+), i\theta^2 J_3] \\ &= -\tfrac{i}{2}\theta^3[e^{i\varphi}J_- - e^{-i\varphi}J_+, J_3] \\ &= -\tfrac{i}{2}\theta^3(e^{i\varphi}J_- + e^{-i\varphi}J_+) \\ &= -\theta^2\partial_\varphi B.\end{aligned} \tag{A.49}$$

Hence, the sum over even-order terms in Eq. (A.4) is

$$\begin{aligned}\sum_{l:\mathrm{even}} \frac{1}{(l+1)!}(\mathrm{ad}_{-B})^l(\partial_\varphi B) &= \partial_\varphi B\left(1 + \tfrac{1}{3!}(-\theta^2) + \tfrac{1}{5!}\theta^4 + \cdots\right) \\ &= \tfrac{i}{2}(e^{i\varphi}J_- + e^{-i\varphi}J_+)\left(\theta - \tfrac{1}{3!}\theta^3 + \tfrac{1}{5!}\theta^5 - \cdots\right) \\ &= \tfrac{i}{2}(e^{i\varphi}J_- + e^{-i\varphi}J_+)\sin\theta,\end{aligned} \tag{A.50}$$

while the sum over odd-order terms in Eq. (A.4) is

$$\begin{aligned}\sum_{l:\mathrm{odd}} \frac{1}{(l+1)!}(\mathrm{ad}_{-B})^l(\partial_\varphi B) &= i\theta^2 J_3\left(\tfrac{1}{2!} + \tfrac{1}{4!}(-\theta^2) + \tfrac{1}{6!}\theta^4 + \cdots\right) \\ &= iJ_3\left(\tfrac{1}{2!}\theta^2 - \tfrac{1}{4!}\theta^4 + \tfrac{1}{6!}\theta^6 + \cdots\right) \\ &= iJ_3(1-\cos\theta).\end{aligned} \tag{A.51}$$

Combining them, we obtain

$$\begin{aligned}R_N^\dagger(\Omega)\partial_\varphi R_N(\Omega) &= d\exp_{-B}(\partial_\varphi B) \\ &= i(1-\cos\theta)J_3 + \tfrac{i}{2}\sin\theta(e^{i\varphi}J_- + e^{-i\varphi}J_+),\end{aligned} \tag{A.52}$$

which is the same as Eq. (A.43).

The gauge potential in $\mathcal{U}_N$ is calculated as

$$\begin{aligned}iA_{N\theta} &= \langle\, \ell, + \,|\, R_N^\dagger(\Omega)\partial_\theta R_N(\Omega) \,|\, \ell, + \,\rangle \\ &= \langle\, \ell, + \,|\, \tfrac{1}{2}(e^{i\varphi}J_- - e^{-i\varphi}J_+) \,|\, \ell, + \,\rangle = 0,\end{aligned} \tag{A.53}$$

from Eq. (A.47) and

$$\begin{aligned}iA_{N\varphi} &= \langle\, \ell, + \,|\, R_N^\dagger(\Omega)\partial_\varphi R_N(\Omega) \,|\, \ell, + \,\rangle \\ &= i(1-\cos\theta)\,\langle\, \ell, + \,|\, J_3 \,|\, \ell, + \,\rangle = i(1-\cos\theta)(\ell + \tfrac{1}{2}) = \tfrac{i}{2}k(1-\cos\theta),\end{aligned} \tag{A.54}$$

from Eq. (A.52), where we have used $k = 2\ell + 1$. Then, we find

$$A_N = -i \langle \ell, + | R_N^\dagger(\Omega) dR_N(\Omega) | \ell, + \rangle = \tfrac{1}{2} k (1 - \cos\theta) d\varphi. \tag{A.55}$$

For the metric, we need to evaluate

$$C_{Nij}(\Omega) = \langle \ell, + | \partial_i R_N^\dagger(\Omega) \partial_j R_N(\Omega) | \ell, + \rangle, \tag{A.56}$$

in addition to the gauge potential. By using Eqs. (A.41)–(A.44), we obtain

$$\begin{aligned}
C_{N\theta\theta} &= \tfrac{1}{2}(\ell + \tfrac{1}{2}), \\
C_{N\varphi\theta} &= -\tfrac{i}{2}(\ell + \tfrac{1}{2}) \sin\theta, \\
C_{N\theta\varphi} &= \tfrac{i}{2}(\ell + \tfrac{1}{2}) \sin\theta, \\
C_{N\varphi\varphi} &= (\ell + \tfrac{1}{2})^2 (1 - \cos\theta)^2 + \tfrac{1}{2}(\ell + \tfrac{1}{2}) \sin^2\theta.
\end{aligned} \tag{A.57}$$

These are shown as follows:

$$\begin{aligned}
C_{N\theta\theta} &= \langle \ell, + | \partial_\theta R_N^\dagger(\Omega) \partial_\theta R_N(\Omega) | \ell, + \rangle \\
&= -\tfrac{1}{4} \langle \ell, + | \left( e^{i\varphi} J_- - e^{-i\varphi} J_+ \right)^2 | \ell, + \rangle \\
&= \tfrac{1}{4} \langle \ell, + | J_+ J_- | \ell, + \rangle \\
&= \tfrac{1}{4}(2\ell + 1),
\end{aligned} \tag{A.58}$$

where

$$J_+ J_- | \ell, + \rangle = J_+ \left( \sqrt{2\ell} | \ell - 1, + \rangle + | \ell, - \rangle \right) = (2\ell + 1) | \ell, + \rangle, \tag{A.59}$$

has been used.

$$\begin{aligned}
C_{N\varphi\theta} &= \langle \ell, + | \partial_\varphi R_N^\dagger(\Omega) \partial_\theta R_N(\Omega) | \ell, + \rangle \\
&= -\tfrac{1}{2} \langle \ell, + | \left[ i(1 - \cos\theta) J_3 + \tfrac{i}{2} \sin\theta (e^{i\varphi} J_- + e^{-i\varphi} J_+) \right] \left( e^{i\varphi} J_- - e^{-i\varphi} J_+ \right) | \ell, + \rangle \\
&= -\tfrac{1}{2} \langle \ell, + | \tfrac{i}{2} \sin\theta J_+ J_- | \ell, + \rangle \\
&= -\tfrac{i}{4} \sin\theta (2\ell + 1).
\end{aligned} \tag{A.60}$$

$$\begin{aligned}
C_{N\theta\varphi} &= \langle \ell, + | \partial_\theta R_N^\dagger(\Omega) \partial_\varphi R_N(\Omega) | \ell, + \rangle \\
&= -\tfrac{1}{2} \langle \ell, + | \left( e^{i\varphi} J_- - e^{-i\varphi} J_+ \right) \left[ i(1 - \cos\theta) J_3 + \tfrac{i}{2} \sin\theta (e^{i\varphi} J_- + e^{-i\varphi} J_+) \right] | \ell, + \rangle \\
&= \tfrac{1}{2} \langle \ell, + | \tfrac{i}{2} \sin\theta J_+ J_- | \ell, + \rangle \\
&= \tfrac{i}{4} \sin\theta (2\ell + 1).
\end{aligned} \tag{A.61}$$

$$\begin{aligned}
C_{N\varphi\varphi} &= \langle \ell, + | \partial_\varphi R_N^\dagger(\Omega) \partial_\varphi R_N(\Omega) | \ell, + \rangle \\
&= -\langle \ell, + | \left[ i(1 - \cos\theta) J_3 + \tfrac{i}{2} \sin\theta (e^{i\varphi} J_- + e^{-i\varphi} J_+) \right]^2 | \ell, + \rangle \\
&= \langle \ell, + | \left[ (1 - \cos\theta)^2 (J_3)^2 + \tfrac{1}{4} \sin^2\theta J_+ J_- \right] | \ell, + \rangle \\
&= \langle \ell, + | \left[ (1 - \cos\theta)^2 (\ell + \tfrac{1}{2})^2 + \tfrac{1}{4} \sin^2\theta (2\ell + 1) \right] | \ell, + \rangle \\
&= (\ell + \tfrac{1}{2})^2 (1 - \cos\theta)^2 + \tfrac{1}{2}(\ell + \tfrac{1}{2}) \sin^2\theta.
\end{aligned} \tag{A.62}$$

By using these, the components in the metric $g_{ij} = \mathrm{Re}(C_{ij} - A_i A_j)$ are found as

$$\begin{aligned} g_{\theta\theta} &= \tfrac{1}{2}(\ell + \tfrac{1}{2}), \\ g_{\theta\varphi} &= g_{\varphi\theta} = 0, \\ g_{\varphi\varphi} &= \tfrac{1}{2}(\ell + \tfrac{1}{2}) \sin^2\theta. \end{aligned} \tag{A.63}$$

*A.4.2. In the open set $\mathcal{U}_S$*

For the gauge potential $A_S$ in $\mathcal{U}_S$, we use the relation $R_S(\Omega) = R_N(\Omega) e^{-2i\varphi J_3}$ to write

$$\begin{aligned} R_S^\dagger(\Omega) dR_S(\Omega) &= e^{2i\varphi J_3} R_N^\dagger(\Omega) d\left(R_N(\Omega) e^{-2i\varphi J_3}\right) \\ &= e^{2i\varphi J_3}\left(R_N^\dagger(\Omega) dR_N(\Omega)\right) e^{-2i\varphi J_3} + e^{2i\varphi J_3} de^{-2i\varphi J_3}. \end{aligned} \tag{A.64}$$

This expression is valid only for $\mathcal{U}_{NS}$, but once we obtain $A_S$, it should be continued smoothly to the south pole. Then, it is straightforward to show

$$\begin{aligned} A_S &= -i \langle \ell, + | e^{2i\varphi J_3}\left(R_N^\dagger(\Omega) dR_N(\Omega)\right) e^{-2i\varphi J_3} | \ell, + \rangle - i \langle \ell, + | (-2id\varphi J_3) | \ell, + \rangle \\ &= A_N - 2 \langle \ell, + | J_3 | \ell, + \rangle d\varphi \\ &= A_N - 2(\ell + \tfrac{1}{2}) d\varphi \\ &= A_N - k d\varphi \\ &= -\tfrac{1}{2} k (1 + \cos\theta) d\varphi. \end{aligned} \tag{A.65}$$

For the metric, using Eq. (A.64) again, we have the relations

$$\partial_\theta R_S(\Omega) = (\partial_\theta R_N(\Omega)) e^{-2i\varphi J_3}, \quad \partial_\varphi R_S(\Omega) = (\partial_\varphi R_N(\Omega) - 2i R_N(\Omega) J_3) e^{-2i\varphi J_3}. \tag{A.66}$$

Thus, in order to obtain $C_{Sij}$, it is sufficient to evaluate the difference from $C_{Nij}$. Apparently $C_{S\theta\theta} = C_{N\theta\theta}$, and

$$\begin{aligned} C_{S\theta\varphi} &= C_{N\theta\varphi} - 2i \langle \ell, + | \partial_\theta R_N^\dagger R_N J_3 | \ell, + \rangle = C_{N\theta\varphi}, \\ C_{S\varphi\theta} &= C_{N\varphi\theta} + 2i \langle \ell, + | J_3 R_N^\dagger \partial_\theta R_N | \ell, + \rangle = C_{N\varphi\theta}, \\ C_{S\varphi\varphi} &= C_{N\varphi\varphi} + \langle \ell, + | \left[2i(J_3 R_N^\dagger \partial_\varphi R_N - \partial_\varphi R_N^\dagger R_N J_3) + 4(J_3)^2\right] | \ell, + \rangle \\ &= C_{N\varphi\varphi} + 4(\ell + \tfrac{1}{2})^2 [-(1 - \cos\theta) + 1] = C_{N\varphi\varphi} - 2kA_{N\varphi} + k^2. \end{aligned} \tag{A.67}$$

Combining these with $A_{S\theta} = 0$ and $A_{S\varphi} = A_{N\varphi} - k$, we obtain the same metric as in $\mathcal{U}_N$. In particular, the difference in the $g_{\varphi\varphi}$ component vanishes, due to the cancellation of contributions from $C$ and $A$.

## References


[1] E. Witten, Nucl. Phys. B **460**, 335 (1996) [arXiv:hep-th/9510135] [Search INSPIRE].
[2] A. Connes, M. R. Douglas, and A. Schwarz, J. High Energy Phys. **9802**, 003 (1998) [arXiv:hep-th/9711162] [Search INSPIRE].
[3] T. Banks, W. Fischler, S. H. Shenker, and L. Susskind, Phys. Rev. D **55**, 5112 (1997) [arXiv:hep-th/9610043] [Search INSPIRE].

[4] N. Ishibashi, H. Kawai, Y. Kitazawa, and A. Tsuchiya, Nucl. Phys. B **498**, 467 (1997) [arXiv:hep-th/9612115] [Search INSPIRE].
[5] H. Aoki, N. Ishibashi, S. Iso, H. Kawai, Y. Kitazawa, and T. Tada, Nucl. Phys. B **565**, 176 (2000) [arXiv:hep-th/9908141] [Search INSPIRE].
[6] R. C. Myers, J. High Energy Phys. **9912**, 022 (1999) [arXiv:hep-th/9910053] [Search INSPIRE].
[7] K. Hashimoto, J. High Energy Phys. **0404**, 004 (2004) [arXiv:hep-th/0401043] [Search INSPIRE].
[8] W. Taylor IV and M. Van Raamsdonk, Nucl. Phys. B **573**, 703 (2000) [arXiv:hep-th/9910052] [Search INSPIRE].
[9] W. Taylor IV and M. Van Raamsdonk, Nucl. Phys. B **558**, 63 (1999) [arXiv:hep-th/9904095] [Search INSPIRE].
[10] T. Azeyanagi, M. Hanada, T. Hirata, and H. Shimada, J. High Energy Phys. **0903**, 121 (2009) [arXiv:0901.4073 [hep-th]] [Search INSPIRE].
[11] T. Hotta, J. Nishimura, and A. Tsuchiya, Nucl. Phys. B **545**, 543 (1999) [arXiv:hep-th/9811220] [Search INSPIRE].
[12] D. Berenstein and E. Dzienkowski, Phys. Rev. D **86**, 086001 (2012) [arXiv:1204.2788 [hep-th]] [Search INSPIRE].
[13] M. H. de Badyn, J. L. Karczmarek, P. Sabella-Garnier, and K. H.-C. Yeh, J. High Energy Phys. **1511**, 089 (2015) [arXiv:1506.02035 [hep-th]] [Search INSPIRE].
[14] M. M. Sheikh-Jabbari, J. High Energy Phys. **0409**, 017 (2004) [arXiv:hep-th/0406214] [Search INSPIRE].
[15] M. M. Sheikh-Jabbari and M. Torabian, J. High Energy Phys. **0504**, 001 (2005) [arXiv:hep-th/0501001] [Search INSPIRE]
[16] J. L. Karczmarek and K. H.-C. Yeh, J. High Energy Phys. **1511**, 146 (2015) [arXiv:1506.07188 [hep-th]] [Search INSPIRE].
[17] G. Ishiki, Phys. Rev. D **92**, 046009 (2015) [arXiv:1503.01230 [hep-th]] [Search INSPIRE].
[18] G. Ishiki, T. Matsumoto, and H. Muraki, J. High Energy Phys. **1608**, 42 (2016) [arXiv:1603.09146 [hep-th]] [Search INSPIRE].
[19] L. Schneiderbauer and H. C. Steinacker, J. Phys. A: Math. Theor. **49**, 285301 (2016) [arXiv:1601.08007v1 [hep-th]] [Search INSPIRE].
[20] A. B. Hammou, M. Lagraa, and M. M. Sheikh-Jabbari, Phys. Rev. D **66**, 025025 (2002) [arXiv:hep-th/0110291] [Search INSPIRE].
[21] A. Sen, J. High Energy Phys. **9808**, 012 (1998) [arXiv:hep-th/9805170] [Search INSPIRE].
[22] A. Sen, Class. Quantum Grav. **17**, 1251 (2000) [arXiv:hep-th/9904207] [Search INSPIRE].
[23] S. Terashima, J. High Energy Phys. **0510**, 043 (2005) [arXiv:hep-th/0505184] [Search INSPIRE].
[24] K. Hashimoto and S. Terashima, J. High Energy Phys. **0509**, 055 (2009) [arXiv:hep-th/0507078] [Search INSPIRE].
[25] K. Hashimoto and S. Terashima, J. High Energy Phys. **0602**, 018 (2006) [arXiv:hep-th/0511297] [Search INSPIRE].
[26] T. Asakawa and S. Matsuura, Prog. Theor. Exp. Phys. **2018**, 033B01 (2018) [arXiv:1703.10352 [hep-th]] [Search INSPIRE].
[27] S. Terashima, arXiv:1804.00647 [hep-th] [Search INSPIRE].
[28] T. Takayanagi, S. Terashima, and T. Uesugi, J. High Energy Phys. **0103**, 019 (2001) [arXiv:hep-th/0012210] [Search INSPIRE].
[29] P. Kraus and F. Larsen, Phys. Rev. D **63**, 106004 (2001) [arXiv:hep-th/0012198] [Search INSPIRE].
[30] M. F. Atiyah, R. Bott, and A. Shapiro, Topology **3**, 3 (1964).
[31] E. Witten, J. High Energy Phys. **9812**, 019 (1998) [arXiv:hep-th/9810188] [Search INSPIRE].
[32] T. Asakawa, S. Sugimoto, and S. Terashima, J. High Energy Phys. **0302**, 011 (2003) [arXiv:hep-th/0212188] [Search INSPIRE].
[33] J. P. Gazeau, *Coherent States in Quantum Physics* (Wiley, Weinheim, 2009).
[34] N. Ishibashi, Nucl. Phys. B **539**, 107 (1999) [arXiv:hep-th/9804163] [Search INSPIRE],
[35] N. Ishibashi, arXiv:hep-th/9909176 [Search INSPIRE].
[36] J. Madore, Class. Quantum Grav. **9**, 69 (1992).
[37] T. T. Wu and C. N. Yang, Nucl. Phys. B **107**, 365 (1976).
[38] P. Baum and R. G. Douglas, Proc. Symp. Pure Math. **38**, 117 (1982).
[39] T. Asakawa, S. Sugimoto, and S. Terashima, J. High Energy Phys. **0203**, 034 (2002) [arXiv:hep-th/0108085] [Search INSPIRE].

[40] V. Periwal, J. High Energy Phys. **0007**, 041 (2000) [arXiv:hep-th/0006223] [Search INSPIRE].
[41] J. A. Harvey and G. Moore, J. Math. Phys. **42**, 2765 (2001) [arXiv:hep-th/0009030] [Search INSPIRE].
[42] R. J. Szabo, Mod. Phys. Lett. A **17**, 2297 (2002) [arXiv:hep-th/0209210] [Search INSPIRE].
[43] R. M. G. Reis and R. J. Szabo, Commun. Math. Phys. **266**, 71 (2006) [arXiv:hep-th/0507043] [Search INSPIRE].
[44] B. Jia, arXiv:1306.0535 [math.KT] [Search INSPIRE].
[45] P. Baum, Proc. Symp. Pure Math. **81**, 81 (2010).
[46] M. R. Douglas, arXiv:hep-th/9512077 [Search INSPIRE].
[47] J. P. Provost and G. Vallee, Commun. Math. Phys. **76**, 289 (1980).
[48] P. Zanardi, P. Giorda, and M. Cozzini, Phys. Rev. Lett. **99**, 100603 (2007) [arXiv:quant-ph/0701061].
[49] N. Seiberg and E. Witten, J. High Energy Phys. **9909**, 032 (1999) [arXiv:hep-th/9908142] [Search INSPIRE].